

**STRENGTH DEGRADATION UNDER 'FATIGUE' STIPULATION  
IN BULK-FILL COMPOSITES: AN IN VITRO APPRAISAL**

**SHRUTI VIDHAWAN AGARWALLA, BDS**

**A THESIS SUBMITTED**

**FOR THE DEGREE OF MASTER OF SCIENCE**

**FACULTY OF DENTISTRY**

**NATIONAL UNIVERSITY OF SINGAPORE**

**2015**

## **DECLARATION**

I hereby declare that the thesis is my original work and it has been written by me in its entirety. I have duly acknowledged all sources of information which have been used in the thesis.

This thesis has also not been submitted for any degree in any university previously.

---

Shruti Vidhawan Agarwalla

24<sup>th</sup> December 2015

*“Good is not good enough, when one aspires for the best;  
strive to push beyond your limit.....”*



## DEDICATION

To **God** for always guiding and blessing me throughout my life and without the grace of whom this would never be possible

To **My Mother**, my pillar of support and strength, for her love and care and whose prayers have always protected me.

To **My Father**, my idol, who has encouraged me to do my best and always believed in me.

To my **Husband**, for supporting me unconditionally to follow my dreams and encourage me to further my education. This would have never been possible without your unwaivered love.

I especially dedicate this thesis, to my **son, Shaurya** for being my angel, for his unconditional love and understanding.

To my **Friends** and **Family** for wishing me infinite success.

National University of Singapore

AY 2014-2016

# Acknowledgement

I would like to express my deepest gratitude to my mentor, Dr. Vinicius Rosa. Thank you for your invaluable knowledge and unprecedented guidance, helping me make the most appropriate decisions and above all, your unconditional support and confidence towards me. It is your continuous encouragement; patience and belief in pushing me farther than I thought I could go, which made it possible to achieve the accomplishments during this period of time. I am grateful for all the time and care that you have given me. You set an example of a best mentor for imparting your precision and passion. You are truly my inspiration.

I would like to deeply thank A/Prof Yap, my co-mentor in this project, for sharing his phenomenal knowledge. Thank you for helping me to think clearly and continuous guidance and stimulation.

I would like to acknowledge Mr Chan Swee Heng for his generous help, his technical advice and guidance and Ms Angeline Han Tok Lin for her support while using the lab.

I would like to show my sincere appreciation to Ms. Nurazreen Binte Mohamed Zaid, for all the help and assistance she has offered to me throughout.

I would like to show my sincere appreciation to Agnieszka Banas and Krzysztof Banas at Singapore Synchrotron Light Source, NUS, for all their help and support. Working with you has been so elevating and a learning growth for me.

I would like to thank all my group members: Xie, Thulasi, Nilesh, Sneha and Ricardo Bentini for their encouragement and continuous support. It was always inspiring working together and your friendship is valued. So proud to 'Be Smart'.

I would also like to thank all my friends and colleagues in the lab. They have been a source of encouragement and have always helped me out at all times.

I want to specially thank Xie, your friendship is truly cherished. All the experiences shared together are enriching and unforgettable.

I want to especially mention, Thulasi and Nandita for giving me their precious friendships and being my moral support. This time wouldn't have been the same without you.

I want to thank Nilesh and Harish for all their support and always bringing in the lighter moments together.

A very very special and distinctive mention to Juliana Colpani, for her unwavering care and support at all times. Thank you for always being there and being an integral part of this journey.

To each and every person, who directly or indirectly has been a part of this journey, Thank you for all your support and input.

# Table of Contents

---

SUMMARY .....	viii
LIST OF TABLES .....	x
LIST OF FIGURES .....	xi
<b>CHAPTER 1: INTRODUCTION</b> .....	1
<b>CHAPTER 2: LITERATURE REVIEW</b> .....	5
2.1: Bulk-fill resin composites .....	5
2.2: Weibull Analysis .....	15
2.3: Fatigue Degradation .....	23
2.3.1: Fatigue Failure .....	23
2.3.1: Slow Crack Growth resistance .....	25
<b>CHAPTER 3: AIMS AND HYPOTHESIS</b> .....	31
3.1: Aims .....	31
3.2: Hypothesis .....	31
<b>CHAPTER 4: MATERIALS AND METHODS</b> .....	32
4.1: Resin Composite materials tested .....	32
4.2: Specimen fabrication .....	34
4.3: Degree of conversion .....	35
4.4: Dynamic fatigue test .....	36
4.5: Weibull analysis and Strength-probability-time diagram .....	40
<b>CHAPTER 5: RESULTS</b> .....	42
5.1: Dynamic fatigue test .....	42
5.2: Weibull analysis and Strength-probability-time diagram .....	48

<b>CHAPTER 6: DISCUSSION</b> .....	53
<b>CHAPTER 7: CONCLUSION</b> .....	59
<b>REFERENCES</b> .....	60



# Summary

---

*Objectives.* The aim of this study was to determine the Weibull and slow crack growth (SCG) parameters of bulk-fill resin based composites. The strength degradation over time of the materials was also assessed by strength-probability-time (SPT) analysis.

*Methods.* Three bulk-fill [Tetric EvoCeram Bulk Fill (TBF); X-tra fil (XTR); Filtek Bulk-fill flow- able (BFL)] and a conventional one [Filtek Z250 (Z250)] were studied. Seventy five disk-shaped specimens (12 mm in diameter and 1 mm thick) were prepared by inserting the uncured composites in a stainless steel split mold followed by photoactivation ( $1200\text{mW}/\text{cm}^2/20\text{s}$ ) and storage in distilled water ( $37^\circ\text{C}/24\text{ h}$ ). Degree of conversion was evaluated in five specimens by analysis of FT-IR spectra obtained in the mid-IR region. The SCG parameters  $n$  (stress corrosion susceptibility coefficient) and  $\sigma_{f0}$  (scaling parameter) were obtained by testing ten specimens in each of the five stress rates:  $10^{-2}$ ,  $10^{-1}$ ,  $10^0$ ,  $10^1$  and  $10^2$  MPa/s using a piston-on- three-balls device. Weibull parameter  $m$  (Weibull modulus) and  $\sigma_0$  (characteristic strength) were obtained by testing additional 20 specimens at 1 MPa/s. Strength–probability–time (SPT) diagrams were constructed by merging SCG and Weibull parameters.

*Results.* BFL and TBF presented higher  $n$  values, respectively (40.1 and 25.5). Z250 showed the highest (157.02 MPa) and TBF the lowest (110.90 MPa)  $\sigma_{f0}$  value.

Weibull analysis showed  $m$  (Weibull modulus) of 9.7, 8.6, 9.7 and 8.9 for TBF, BFL, XTR and Z250, respectively. SPT diagram for 5% probability of failure showed strength decrease of 18% for BFL, 25% for TBF, 32% for XTR and 36% for Z250, respectively, after 5 years as compared to 1 year.

*Significance.* The reliability and decadence of strength over time for bulk-fill resin composites studied are, at least, comparable to conventional composites. BFL shows the highest fatigue resistance under all simulations followed by TBF, while XTR was at par with Z250.

Keywords: Dynamic fatigue, Strength degradation, Subcritical crack growth, Weibull analysis, Strength–probability–time diagram, Resin composites

# List of Tables

---

<b>Table 2.1</b>	Mean DC of materials immediately post-cure and 24h post-cure.....	7
<b>Table 2.2.</b>	Results of Weibull parameters (Weibull modulus, m; characteristic strength, $\sigma_0$ ) different resin based composites studies.....	21
<b>Table 2.3.</b>	Subcritical crack growth parameters of different dental restorative materials.....	29
<b>Table 4.1.</b>	Chemical composition of matrix, filler and filler content by weight (Wt%) and volume (Vol%) of resin composites used as by manufacturer.....	34
<b>Table 5.1.</b>	Biaxial flexural strength (in Mpa) and standard deviation (in parenthesis) of all the materials tested.....	42
<b>Table 5.2.</b>	Degree of conversion after 24 hours (DOC), n (subcritical crackgrowth susceptibility coefficient) and $\sigma_{f0}$ (scaling parameter), with respective standard deviations in parenthesis.....	45
<b>Table 5.3.</b>	Fracture stresses (MPa) estimated for 1 day ( $\sigma_{1d}$ ), 1 year ( $\sigma_{1y}$ ) and 5 years ( $\sigma_{5y}$ ).....	47
<b>Table 5.4.</b>	Weibull modulus (m), characteristic strength ( $\sigma_0$ ) and 95% confidence intervals in parenthesis.....	49
<b>Table 5.5.</b>	Reliability probability over time – Strength at more clinically relevant failure probability of 5% at different times for all the composite materials.....	52

# List of Figures

---

<b>Figure 2.1.</b> Mean volumetric shrinkage values for each material tested.....	10
<b>Figure 2.2.</b> Failure probability of a ceramic as a function of stress (normalized in terms of $\sigma_0$ ). Large values of the Weibull parameter m indicate a small variability in strength.....	18
<b>Figure 2.3.</b> Weibull plot showing effect of ion exchange in porcelain.....	20
<b>Figure 2.4.</b> Slow crack growth in oxide ceramics is caused by the hydration of the M-O bond.....	26
<b>Figure 4.1.</b> Tetric EvoCeram Bulk-fill resin composite.....	32
<b>Figure 4.2.</b> X-tra fil Bulk-fill resin composite.....	32
<b>Figure 4.3.</b> Filtek Bulk-fill resin composite (flowable).....	33
<b>Figure 4.4.</b> Filtek Z250 (conventional composite).....	33
<b>Figure 4.5.</b> MIRacle (PIKE, USA) – High Throughput and Efficient Optical Design.....	36
<b>Figure 4.6.</b> Biaxial flexure strength test set up.....	37
<b>Figure 4.7.</b> Axial view of schematic drawing of piston-on-three-ball setting for biaxial flexural test.....	38
<b>Figure 4.8.</b> Coronal view of schematic drawing of piston-on-three-balls setting for biaxial flexural test.....	38
<b>Figure 5.1.</b> Flexural strength as a function of stress rate of the materials tested.....	43

<b>Figure 5.2.</b>	Time taken to fracture each specimen at given stress rates for all materials tested respectively.....	44
<b>Figure 5.3.</b>	Lifetime curve the log of flexural strength (in MPa) to the log of time of fracture. The time axis is labeled for 1 day,1 year and 5 years.....	46
<b>Figure 5.4.</b>	Weibull plot of the flexural strength test for the tested group of materials.....	49
<b>Figure 5.5.</b>	SPT diagram all the composites tested. The lines correspond to the fracture stresses ( $\sigma_a$ ) for the time of failure of 1 year and 5 years.....	51

# Chapter 1

## Introduction

---

Bulk-fill resin composites were introduced with claims of time saving through up to 4 mm thick placements that can be photopolymerized in one step during restoration. As increment size variability depends on the skill level of clinicians (1), these materials can conceivably overcome problems related to traditional layering techniques such as the presence of voids or contamination between layers (2).

The physical, chemical and mechanical properties of bulk-fill resin composites have been comprehensively studied. These materials may present degree of conversion (DOC) as high as 76% to 86% at 1 mm reaching up to 64% at 4 mm depth which is similar to conventional resin composites in the 55–60% range at 1 mm (3-7). It has been found that the marginal quality to enamel and dentine as well as internal dentine adaptation of bulk-fill resin composites is similar to conventional composites (8, 9). Moreover, bulk-fill resin composites exhibit nanoindentation and bulk compressive creep analogous to conventional resin composites (10, 11). On the contrary, it is seemingly impossible to generalize the entire class of material as the elastic modulus and flexural strength of bulk-fill resin composites differs as a function of the resin formulation, filler type and loading. The elastic modulus of bulk-fill resin composites can vary from 3.3 to 9.4 GPa (7). Higher elastic modulus were reported

for some bulk-fill composites (~15 GPa) but the values obtained were lower than that measured for conventional resin composites (up to 20 GPa) (12).

Some studies have reported significant variations when comparing the physical and mechanical properties of various bulk-fill resin composites and conventional composites (3, 7). Nonetheless some have not established discrepancy in the flexural strength while paralleling different bulk-fill resin composites (5, 13). However, fracture strength per se, cannot predict structural failure as it specifies only perception into the stresses that the material will endure (14). Alternatively, Weibull distribution, takes into consideration the scatter in strength measurements to describe the reliability of materials (i.e. stress required to fracture a given percentage of specimens) as they are scaled-up in size (larger volume or surface under stress) (4, 15, 16). Weibull analysis dictates the probability of fracture of brittle materials as a function of applied stress. Weibull modulus ( $m$ ) represents the reliability of the material based on its flaw distribution, derived from the Weibull analysis which integrates the failure probability ( $P_f$ ) of a material analogous of the stress values ( $\sigma_f$ ), emerging closer to interpret the population of defects in a specimen (17-19).

The aim of any *in-vitro* studies are definitely in concurrence with clinical performance of dental materials and aiding to make materials serve better and longer in the oral environments. Furthermore, the strength of many brittle materials is environment and time-dependent (19, 20).

The oral environment plays a very important role due to its complexed fatigue scenario and plays a critical role in the degradation of the restorative materials. Chemical exposure, Cyclic masticatory forces, Corrosive water attack and local stresses all impact resin composite material during its service life in the oral

environment. The degradation of resin based composite restorations ensues in-service, due to hydrolytic degradation by moisture (21, 22), saliva introduces enzymatic degradation (23, 24), and degradation by regularly consumed food substances (25, 26). The manifestation of water has been shown to degrade the mechanical properties of resin based composite restorations through a time-dependent process relative to the degree of water sorption of the material. Thus the very aspect of fatigue resistance of the bulk-fill materials and simulations of their performance can provide an insight about the strength degradation of the materials over time.

The strength degradation over time is related to the material's susceptibility to slow crack growth (SCG) (14, 19). SCG is the formation and extension of cracks over time at stress levels below that causing immediate failure to occur in the presence of a reactive medium, especially water (27). This susceptibility to SCG, is expressed in a material by the stress corrosion coefficient ( $n$ ), and the material's endurance in the initial phases of mechanical loading ( $\sigma_{f0}$ ) which can be determined by direct and indirect in vitro methods (18). The dynamic fatigue test is an indirect way to determine these parameters ( $n$  and  $\sigma_{f0}$ ) that relies on mathematical relationships among fracture resistance values, attained at different stress rates (18-20, 28, 29).

By combining the SCG parameters (which presents the time dependency of strength) to the Weibull parameters (used to describe strength variability of brittle materials) it is possible to obtain the strength-probability-time (SPT) diagrams. This SPT diagram, allows the estimation of a material's failure probability over its lifetime for a specified stress level (18, 19).

The degradation and subsequent failure of composite restorations is an intricate and multi-factorial process involving both physical and chemical factors.



Clinically, resin composites must have high fracture resistance and also a low propensity of strength degradation over time. The mechanical tests and qualitative analysis must mimic the oral environment and would be pivotal to assess the longevity of composite restorations as well due to flaw distribution and the initiation of the SCG. Although, there is a lot of literature available on bulk-fill composites, there is currently no information to show their strength degradation and reliability over time under fatigue conditions.

## Chapter 2

# Literature Review

---

### 2.1 Bulk-fill resin composites

The clinical selection of restorative materials requires the balancing of various requirements. Over the years, the longer clinical durability (30) and ease of handling attributed to ‘packability’ and ‘condensability’ (31, 32) has favoured the use of dental amalgam. However, the use of amalgam has declined in current past. Tooth colored materials including resin based composites have been developed and constantly improved upon.

The various reasons for this reasonably prompt and noteworthy change in restorative dentistry in favor of the resin based composites include the: (i) higher esthetic demands from patients and awareness of mercury toxicity, further in-situ (ii) the less invasive nature of composite restorations (33) (iii) significant advances in composite resin material physical properties, leading to increased durability and longevity (34, 35). Dental resin-based composites however, have several disadvantages. These include polymerization shrinkage, limited depth of cure, and lower physico-mechanical properties when compared to amalgam (36). In addition they are also technique sensitive, and the restorations are time consuming to place clinically.

Ideally, resin based composites should allow ease of use and placement in ‘bulk’ increments, high degree of conversion (DOC), with low polymerization shrinkage and sufficient mechanical properties to withstand occlusal loads. Depths of cure should also be more in contrast to the maximum 2 mm increments advocated for conventional resin composites (8, 15, 37). Bulk-fill resin composites thus, have been pronounced as the “new-class” of dental restorative resin composites. The problems related to traditional layering techniques such as the presence of voids or contamination between layers can probably be minimized (2). The number of increments being vital to fill a cavity, and as only one increment is needed to fill a cavity, the material and technique simplifies restorative procedures and saves clinical time.

Several studies were conducted to evaluate the physical and mechanical properties for a range of bulk-fill resin composite materials. The depth of cure of bulk-filled composites was determined by measuring hardness and degree of conversion (4).

Degree of conversion (DOC) is a critical parameter in determining the physical, mechanical performance and biocompatibility of photo-activated composite resins (38). The DOC is determined by the proportion of residual concentration of the aliphatic C=C double bonds in a cured sample in relation to the total number of C=C bonds in the uncured material. Fourier Transform Infra-red Spectroscopy (FT-IR) is one of the most used techniques for measurement of DOC in dental composites (39, 40). Strength, modulus, hardness and solubility obtained have been directly correlated to the degree of conversion (41-43).

The degree of conversion has a key influence on the fundamental success

of a resin composite restoration (44, 45) and ample polymerization results in improved physical properties (46). The claim of clinically acceptable DOC in bulk-fill resin composites up to depths of 4 mm has been supported in current literature (5, 6, 47). Bulk-fill materials may present DOC as high as 76% to 86% at 1 mm reaching up to 64% at 4 mm depth similar to conventional resin composites in the 55–60% range at 1 mm (4-8). Comparable results between the conventional composites and the bulk-fill resin composites were reported at two time intervals as shown in Table 2.1 (5). Intriguingly another study shows the mean DOC at 24 hours post cure of bulk-fill composites at 4 mm (55.6% to 83.3%) was comparable to that of conventional composites at 1 mm (68.6% to 78.1%) (6).

Table 2.1. Mean DC of materials immediately post-cure and 24h post-cure [Adapted from Alshali et al, 2013].

Material	Types	DOC% (immediately post-cure)	DOC% (24h post-cure)
Surefil SDR	Bulk-fill resin composites	58.4	76.1
Venus Bulk-fill		55.7	79.2
X-tra base		53.9	62.1
Filtek Bulk-fill		49.5	50.9
Venus Diamond flow	Conventional composites	62.0	70.6
Venus Diamond		34.7	79.0
Grandioso		50.0	69.1

DOC of resin composites can be influenced by various factors like filler particle size and loading, polymerization initiator concentration (48, 49), translucency of the material and monomer type and amount (50), intensity and wavelength of the light source, as well as irradiation time (51).

The improved degree of conversion of the bulk-fill resin composites, can be attributed to both improvements in photo-initiator dynamics and their amplified translucency, which permits additional light penetration and a deeper cure (52-54). In general, bulk-fills present a higher translucency than conventional resin composites (55). Translucencies of Tetric bulk-fill 15%, QuixFil 17%, X-tra Fil 23% were reported for the bulk-fill resin composites (56). These values are higher than the ones reported for conventional Tetric EvoCeram at 10% (56) and Filtek Z350 around 11% (57)

There is a strong link between light transmission and material's translucency (58). Thus the desired %DOC at 4 mm depth for the bulk-fill resin composites may be influenced by the reduced opacity (59). Recent studies revealed that reduction in filler content can also enhance translucency (60). It appears that reducing filler content together with increasing filler size plays a critical role in attaining higher translucency of bulk-fill resin composites (55). It has been shown that bulk fill with low filler content can present higher DOC (ranging from 43 to 65%) as compared to conventional composites at 2 mm depth (38%) (59).

DOC is commonly measured to estimate photo-polymerization efficiency by spectroscopic techniques (61, 62). The DOC was determined by FTIR, with the hardness being measured, in clinical relevant filling depths (0.1, 2, and 4 mm; 6 mm bulk incremental) and different irradiation times (10, 20, 40 s) (15). In this study, the bulk-fill resin composites tested [Surefil SDR and Venus bulk-fill] showed, similar DOC for different irradiation times as well at different depths. For both the materials at the clinical relevant depth of 4 mm the DOC recorded for 10s and 40s irradiation times ranged from 58 to 66% (15). Within the limitation of the study the results were in the consensus of the DOC at 4 mm, was comparable to the conventional composites at 1mm (55 to 60% DOC).

Another important property asserted by bulk-fill resin composites, that allows them to be placed in material increments up to 4 mm in thickness without negatively affecting degree of conversion (3), is their low volumetric polymerization shrinkage and low polymerization shrinkage stress (63-66).

The polymerization shrinkage of dental resin composites is due to the suitable conversion of monomers in polymers. This polymerization shrinkage creates shrinkage stresses in the restoration and internal stress (67-71). The shrinkage stress of resin-based composites can affect marginal integrity and lead to marginal leakage, debonding, secondary caries, post-operative sensitivity, cusp deflection in high C-factor in direct composite restorations (10, 15, 72-76). While polymerization shrinkage is the reason, shrinkage stress can be perceived as the mechanism and thus, aids in the restoration to possess apt physical, chemical and mechanical properties in clinical dentistry (68, 77-82).

The development of low-shrinkage composites has been the object of much developmental work. Some bulk-fill resin composites present lower polymerization shrinkage when compared to conventional composites (72). The mean volumetric shrinkage values of some bulk-fill resin composites (Tetric bulk-fill, SonicFill, Quixfil and x-tra fil) at 4 mm increment ranged as low as 1.86-1.96% (63). Volumetric shrinkage was lower than conventional composites that ranged from 3% to 6% (67, 83-85). Another study evaluating polymerization shrinkage for some bulk-fill resin composites as shown in Figure 2.1, however reported values (3.43% to 4.40%) which were in similar range to conventional composites (3% to 6%) (8).

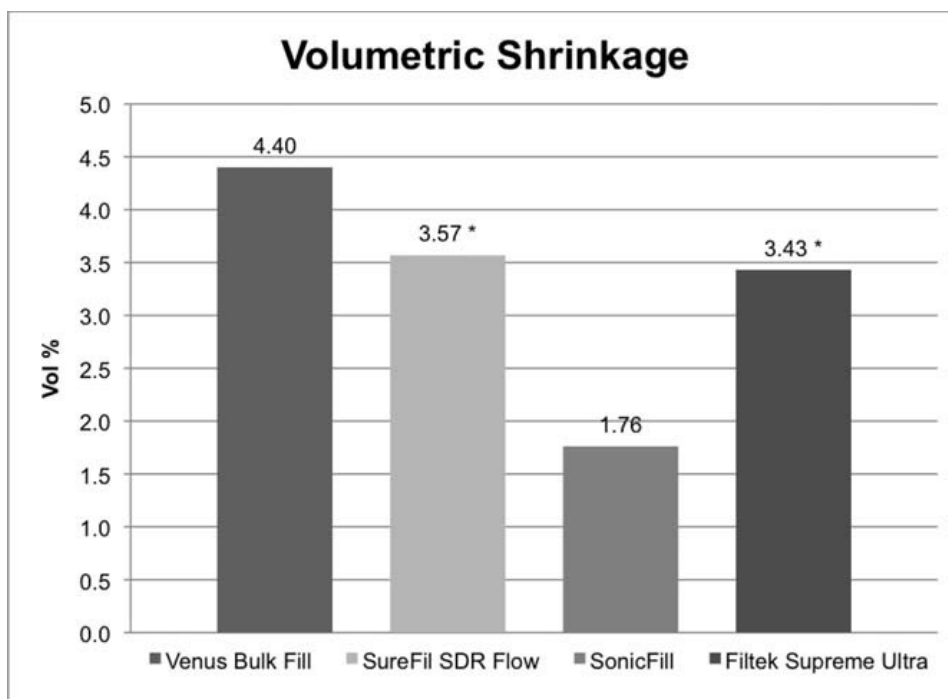


Figure 2.1. Mean volumetric shrinkage values for each material tested. Values with an (\*) were not significantly different [Adapted from D Garcia et. al., 2014].

Another strategy created for new resin systems for minimizing shrinkage and facilitating bulk placement is the development of stress-decreasing resin technology (8). These new resin technologies allows a certain amount of flexibility and optimized network structure during polymerization (86). To enhance properties of the bulk-fill resin composite, manufacturers integrated new pre-polymer shrinkage stress relievers and polymerization modulators in Tetric bulk-fill to reduce polymerization shrinkage stress that facilitates the use for single incremental layering (72, 87-89). This eventually also leads to comparable (9, 10) or enhanced (90) changes in the cervical microleakage, and significantly reduced cuspal deflection (4, 91, 92).

Hardness is an indirect method to measuring depth of cure (41, 93). Usually a good linear correlation has been observed between depth of cure and microhardness (54). Generally, an indication of adequate cure is when the hardness of the bottom surface of materials reaches 80% of its surface hardness (94, 95) or, further conservatively, 80% of its maximum hardness (47).

Investigations using hardness depth profiles and top to bottom hardness ratio, have shown adequate cure at depths up to 5 mm for bulk-fill resin composite materials (47, 55), comparable to conventional composites at 2 mm depths (96). The hardness profiles presented in different studies with respect to several bulk-fill resin composites such as X-tra Fil, Venus bulk-fill, SureFil SDR, X-tra base and Filtek bulk-fill (15, 97) presented top to bottom hardness ratio above 80% at 4 mm depth of cure (98). SonicFill had the greatest depth of cure at 5.03 mm followed by Tetric bulk-fill at 4.47 mm at the 80% ratio (47).



The Vicker's Hardness Number (VHN) for bulk-fill resin composites varied from 13.05 to 70.10 (20 s irradiation time), as for conventional it was seen at 55.95 to 68.50 (20 s irradiation time). (54). Although the bulk-fill resin composites were at par with conventional composites, there were differences amongst the various products. For example Tetric EvoCeram bulk fill presented hardness close to conventional Tetric EvoCeram (VHN~50), whereas for Filtek bulk fill (VHN~30) was lower as compared to 60-80 VHN for conventional counterpart Filtek Supreme XT (99). The top to bottom surface Knoop Hardness for bulk-fill resin composites at 4 mm was reported to range from 72.4 to 15.6 KHN. Conventional composites was, however, too soft to be tested at 4 mm (8).

In the available literatures, other interesting characteristics exhibited by bulk-fill resin composites have been reported. They may present similar nanoindentation and bulk compressive creep as conventional resin composites (3, 13). The elastic modulus and flexural strength of bulk-fill resin composites might be affected by variations in the resin formulation and in filler type and loading, making it impossible to generalize the whole class of material. The elastic modulus of bulk-fill composites, for example, has been found to vary from 3.3 to 9.4 GPa (4). Higher elastic modulus was reported for some bulk-fill composites (~15 GPa) but values obtained were lower than conventional ones (16).

Though some studies have not found differences in the flexural strength while comparing bulk-fill resin composites (15, 97) others have reported significant discrepancies when various bulk-fill resin composites and conventional ones were compared (4, 100). The flexural strength of Filtek bulk fill and Venus bulk fill were 88.4 and 76 MPa as compared to 115 to 125 MPa of conventional composites. The flexural strength of SonicFill and x-tra fil was

higher than conventional composites at 140.3 and 130.7 Mpa respectively (4). Furthermore, the flexure strength obtained for Tetric EvoCeram bulk-fill (4) was comparable to its conventional counterpart (~ 90 MPa) (99). There was also a difference shown in the flexure strength while comparing two flowable bulk-fill resin composites SureFill SDR (131.8 MPa) and Venus bulk-fill (122.7 MPa) (15). SureFill again had higher flexure strength when compared to conventional composite (112.64 to 125 MPa) (4, 100), while Venus bulk-fill had comparable strengths.

Since bulk-fill resin composites was introduced importantly with the concept of a single bulk increment restorations, such that it simplifies the clinical procedure and reduces working time. Several studies give us an insight for the physical and mechanical behavior of the new class of bulk-fill resin composites. It is imperative to note that despite having clinically acceptable DOC values at 4mm depth, studies have noticed substantial differences between the various bulk-fill resin composites available in terms of mechanical properties. Much emphasis has been on properties such as indentation modulus, Vicker's hardness, flexural strength, and flexural modulus. However, flexural strength only gives the stress at which the fracture of brittle material will occur. Nonetheless, fracture strength alone cannot predict structural failure as it provides only insight into the stresses that the material will withstand for a given flaw size distribution (14).

Several studies about the bulk-fill resin composites lead to extensive *in-vitro* appraisal of their physical and mechanical behavior. The evaluation of strength would ultimately be assessed critically on the degradation of the

material over time. Thus enabling to reliably predict structural failure. Recognition of this strength degradation helps us prevent catastrophic failures. Thus, investigation of strength degradation over time of bulk-fill resin composites, would be crucial to simulate the structural failure of restorations in clinical consensus.

## **2.2 Weibull Analysis**

The measure of structural performance for brittle dental materials is often based on their strength values. However, predicting structural performance from strength data alone cannot be directly deduced and is more of a “contingent” than an inherent material property. It is mostly observed that dental restorative such as ceramics and composites are susceptible to brittle fractures. Brittle materials, may lead to catastrophic failure prior to detectable deformation due to flaws such as cracks, inclusions and pores and other innate defects that act as stress concentrators. This trait has also caused amplified susceptibility to failure when they are subjected to tensile loading. These failures revealed unfavorable effect on the survival and success as fractures clinically, in restorative dentistry. Thus flaws are not inevitably involuntary defects in a material (101).

The microscopic flaws control strength in brittle materials, was primarily brought into perception from both the theoretical and experimental work of Griffith (1920). The concept shows that increase in cracks in brittle materials arise when the accumulated elastic energy emanated during extension, surpasses the energy enforced to form a alternative facet. Henceforth, testing tensile strength was considered one of the most important physical properties to be tested in dental materials and flexure test, the most commonly used method to evaluate tensile strength (102) which is the standard mean for testing strength of dental composites.

Thus, as fracture strength cannot alone predict the structural failure, the mean strength that has commonly been taken, as a measurement of the robustness of the material does not represent the failure probability with precision. This shows why many brittle materials break randomly, either below or above the mean strength (103). Brittle materials are assumed to have a flaw size distribution following Gaussian distribution in different studies. Conventional mean strength data misjudges the flawed sample population resulting in impending fracture at a significantly lower load range and risk early failure. In the understanding of this restraint, a statistical method consenting more accurate characterization of material strength is sought. The application of Weibull analysis introduced, was believed to provide a robust theoretical foundation (101).

Weibull analysis is a reliability and probability function to anticipate and account the wear-out of the material, particularly focused on failure-rate. The crucial advantage of Weibull analysis is the capability to stipulate realistically accurate failure analysis and failure forecasts with extremely small samples. This makes it particularly valued in dental application, eminently because of the test specimen size restraint (101). Another advantage of Weibull analysis is that it postulates a simple and expedient graphical plot of the failure data.

By using Weibull statistics, the prediction and analysis of fracture strength can be made more realistically. Weibull statistics, takes into consideration the scatter in fracture strength measurements to describe the reliability of materials (i.e. Stress needed to fracture a specified percentage of specimens) as they are scaled-up in size (larger volume or surface under stress) (14, 18, 101). Weibull analysis dictates the probability of fracture of brittle

materials as a function of applied stress. Failure mostly occurs at the weakest point, inside the structure before disseminating to catastrophic failure, this is called the weakest-link principle, on which the Weibull distribution functions.

The Weibull statistics is based in two distinct parameters: Weibull modulus and characteristic strength. The Weibull modulus ( $m$ ) is a dimensionless material-specific parameter that describes the variability of strength of brittle materials. The parameter  $m$  is the slope of the Weibull plot that is used to describe the variation in the strength or asymmetric strength dissemination as a result of defects and microcracks which may develop within the microstructure (104) Thus, low value of the Weibull modulus, indicates more flaws and discrepancies in the material, and hence lower reliability. (104). Since it is inversely related to the standard deviation in a normal distribution, high Weibull modulus relates to higher reliability of materials (27). A higher Weibull modulus equates to a more homogeneous flaw distribution, throughout the entire volume, which result in higher structural reliability and lower failure probability (27, 105-107). The values for  $m$  can range from 5-15 as shown for ceramics, whereas metals, which produce ductile failures, values displayed are in the range of 30-100. The  $m$  values for some bulk-fill composites can vary from 10.4 up to 26.7 (7, 15). Fig. 2.2, depicts the significance of  $m$  value, where the  $m=20$  for ceramics is more vertical as compared to  $m=5$  for pottery and window glass as the results are less scattered. Thus the ceramics show less variability in fracture strength, hence slated as more reliable and can be used in applications under stress (104).

The second parameter, characteristic strength ( $\sigma_0$ ), is a location parameter that corresponds to the stress level for a 63.2% probability of failure (103). Since it is related to the fracture strength of a material, it may vary with specimen geometry and test set-up (14, 27), signifying the position where the strength ( $\sigma$ ) data lies.

In Weibull analysis, the fracture strength is fitted to these two parameters ( $m$  and  $\sigma_0$ ), accumulative probability function is written as such that the fracture probability,  $P_f$ , increases with the fracture stress variable,  $\sigma$ : as shown in Equation 2.1.

$$P_f(\sigma) = 1 - \exp \left[ - \left( \frac{\sigma}{\sigma_0} \right)^m \right] \quad \text{Equation 2.1.}$$

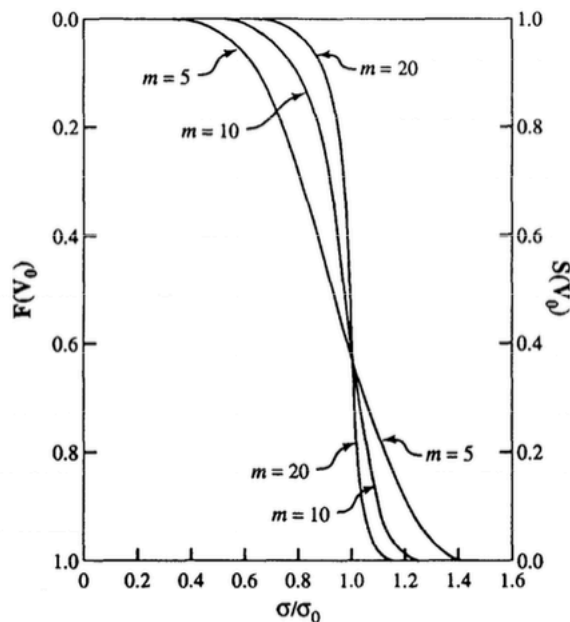


Figure 2.2. - Failure probability of a ceramic as a function of stress (normalized in terms of  $\sigma_0$ ). Large values of the Weibull parameter  $m$  indicate a small variability in strength. [Adapted from Ritter et al., (1995)]

Weibull analysis consents evaluation of measured strengths attained from different stress configurations, test specimen sizes and testing conditions (101). In addition, it stipulates fracture probability and reliability of a material for life time (17). For example in Figure 2.3 below, the Weibull plot shows the characteristic strength ( $\sigma_0$ ) of dental porcelain in different testing conditions. One control group and the other underwent the ion exchange surface treatment. The  $\sigma_0$  for control and ion exchange were 60.4 and 136.8 MPa respectively which makes the ion exchange group having at increase of 126%. On the other hand the m value for ion exchange decreases by 46% having a value of 7.4 in contrast to control representing the m at 13.8 (18). The Weibull plot thus displays that the material which is porcelain itself for both experimental conditions as presented, shows a high variability in the reliability and strength results. It can be deduced that porcelain tested with ion exchange presented a lower reliability but a higher strength respectively.



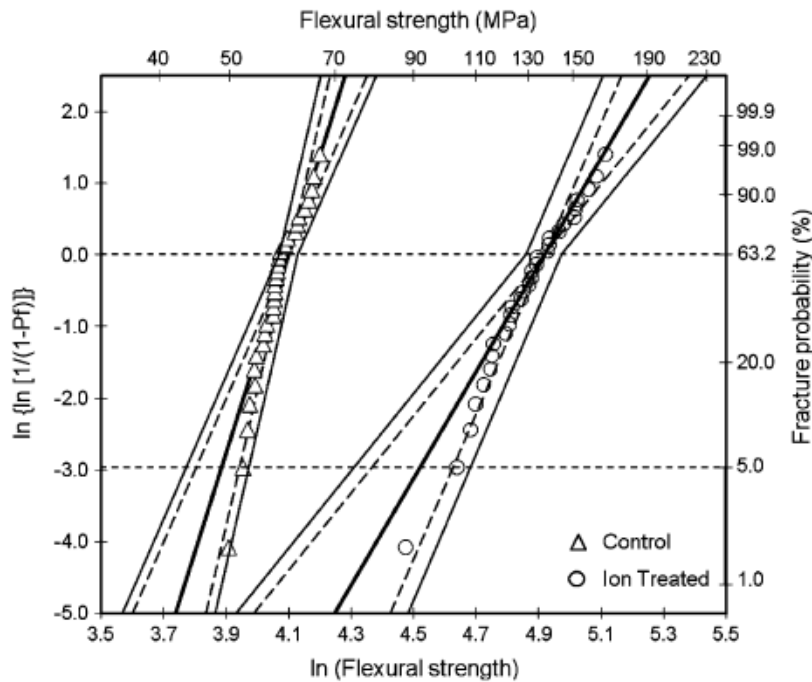


Figure 2.3. Weibull plot showing effect of ion exchange in porcelain. (Adapted from Rosa *et al.*, 2009).

Extrapolating Weibull allows for mechanical assessment of the reliability of the material. It has been conducive in a few studies that the reliability measured for bulk-fill composites by the Weibull analysis have given comparable results to those of conventional composites. Results of Weibull parameters (Weibull modulus,  $m$ ; characteristic strength,  $\sigma_0$ ) from different composites studies is summarised in Table 2.2. These studies while determining the reliability of the resin composite materials tested, show that the Weibull moduli range from 6.6 to 26.6 and characteristic strength range from 104.8 to 169.9 MPa for conventional composites and 120.8 to 137 MPa for bulk-fill resin composites respectively. The  $m$  for bulk-fill composites namely, Surefil SDR and Venus bulk-fill were found to be 26.6 and 21.1 respectively, characterizing a

high weibull modulus ( $m$ ), thereby increased reliability, whereas for conventional composites the  $m$  was between 6.6 to 7.2 (7). This however was unexpected as values for conventional composites were measured between 6.37-15.23 (108).

Table 2.2. Results of Weibull parameters (Weibull modulus,  $m$ ; characteristic strength,  $\sigma_0$ ) different resin based composites studies (Pick et al., 2010 and Ilie et al., 2013).

Study	Year	Materials	Type	$m$	$\sigma_0$ (Mpa)
Pick et al	2010	Concpet Advanced	Conventional composite	8.6	122.4
		Filtek Z250	Conventional composite	6.6	169.9
		Heliomolar	Conventional composite	7.2	104.8
Ilie et al	2013	Tetric Evo Ceram	Bulk-fill composite	11.2	120.8
		Venus Bulk fill	Bulk-fill composite	21.1	122.7
		Surefil SDR flow	Bulk-fill composite	26.6	131.8
		X-tra base	Bulk-fill composite	10.4	137.0

In this perview, a larger Weibull modulus is desirable as it guarantees more uniform performance among different materials (109). This advocates that Weibull analysis aids to provide an ample perspective in comprehending fracture which possibly can enhance dental material selections in situ (101). This will allow for enhanced understanding of material characteristics, leading to better

material selection clinically. The use of Weibull statistics in dental materials science, confirms the use of precise scientific methods to evaluate the functioning of materials, permitting sturdier and robust restorative materials to be developed.

## **2.3 Fatigue degradation**

### **2.3.1 Fatigue failure**

In dentistry, weakening or failure of a material resulting from prolonged stress confounds the fatigue of material. The clinical endurance of restorations after their placement in the oral environment is subjected to fatigue, assisted crack growth and wear resistance. Clinical substantiation on the functioning resin composite restorations points to fracture as one of the 2 core factors leading to clinical failure. Clinically, an accretion of the microstructure damage during mastication may provoke a catastrophic failure.

Subsequently, restorative materials susceptible to such degradation mechanisms exhibit a weakening, leading to catastrophic failure under prolonged stress. Thus, elevated force and recurring stresses during chewing cycles may lead to fatigue of the material and premature fracture in the oral environment. Therefore, fatigue is a vital characteristic of clinical performance of restorations.

Fatigue, hence is another mode to appraise the mechanical performance of a material. Fatigue is the manner of failure; whereby a structure ultimately fails after being repetitively imperiled to stress that is so small that one application does not cause failure. A modus where the material undergoes mechanical degradation below critical failure stress and involves the subcritical flaws at subcritical loads. Which in turn refers to the slow growth of cracks, facilitated by the blend of water and stress (110). The impact of water and fatigue initiated by cyclic loading in the oral environment, such as mastication, are

essential factors in the long-term endurance of dental restorations (111). It has been accepted that the presence of water will lower the strength of silicate glasses and other ceramic materials (110).

Mostly all, restorative materials are susceptible to fatigue mechanisms that can considerably reduce their strength over time due to the propagation of innate flaws in materials. The deterioration of mechanical strength owing to fatigue is caused by the dissemination of innate cracks initially existing in the component's microstructure (112). It is imperative to know the fracture mechanism in understanding and predicting the life of materials. In the most elementary form, fracture can relate the permissible limit applied loads superseding upon a structural component to the size and location of a crack (either real or hypothetical) in the element (Kanninen and Popelar, 1985). It can also be used to calculate the scale at which a crack can approach a critical size in fatigue or by environmental influences. Fracture arises only when the stress absorption within the material comes to the critical level known as the plain strain fracture toughness, which depicts the ability of a material containing a crack to resist fracture.(113)

Characterization of a material's fracture resistance is vital for screening, however, because that property is largely resolute under static or quasi-static loading and it might not be illustrative of the material's strength when in function (4, 7, 114, 115). Fatigue in restorative materials is influenced by corrosive water attack at a certain temperature and by cyclic masticatory forces that ultimately may lead to strength degradation (18-20, 115-117). The influence of moisture contamination has also previously been identified to affect the fracture strength

of ceramic-based dental ceramics, resulting in a 20% decrease in the mean fracture strength (112). All ceramic crown and bridge restorations are exposed on a daily basis to the complexed oral scenarios that places the restoration under repeated loading throughout its service-life (118).

In line with fatigue principals, current approaches consider a fracture process in three stages: initial crack, slow crack growth, and fast fracture. Initially the crack forms around the discrepancies such as the porosities, filler particles, craze and surface and subsurface microscopic cracks in the material. When subjected to stress intensity at the subcritical stress level materials present a slow and stable growth. Thus, in this way the flaw will ingress and grow slowly until reaching the analytical size of fracture for a given applied stress leading to catastrophic failure (104). The last stage is very brief, thus the time of crack initiation and that of slow crack growth aid for the effective fatigue resistance of a material.

### **2.3.2 Slow crack growth resistance**

The subcritical crack growth signifies to environmentally augmented crack propagation at subcritical stress intensities. The dissemination of the pre-existing natural flaws occurs at muted rates (slow crack growth), and causes delayed failure, when the flaw size reaches a critical value (119). When internal and surface flaws are subjected to the subcritical level, the flaws come into prominence as a slow and stable growth called slow crack growth (SCG). Brittle materials are vulnerable to time-dependent failure under static loads, initiated by the subcritical growth of cracks to perilous lengths (120). The subcritical parameters  $\sigma_{f0}$  and  $n$  are typically examined for estimating crack growth

resistance and lifetime of materials. This is accentuated under moisture environment and especially influences the formation and augmentation of the crack over time. This is especially seen in ceramics when water molecules enter a crack tip that is under stress, causing a chemical reaction between water and ceramic that with subsequent formulation of hydroxides by breaking the metal oxide bonds as shown in Fig. 2.4, leading to strength degradation over time (104)

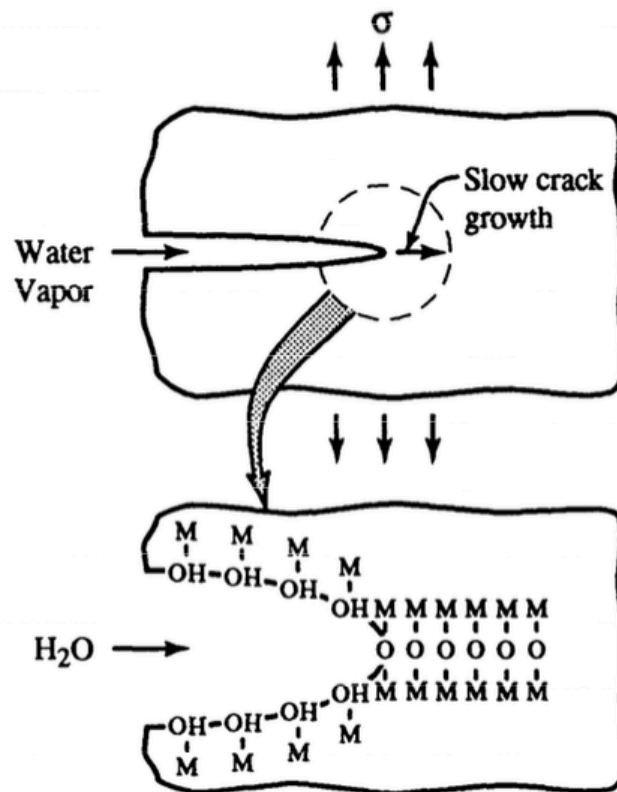


Figure 2.4. - Slow crack growth in oxide ceramics is caused by the hydration of the M-O bond; (Adapted from Ritter et. al, 1995)

In resin composites the exposure to water, accelerates slow crack growth as it causes several weakening effects at the filler-matrix interface, elution, and contusion on the matrix. (116, 117, 121). The Griffith criterion pronounces the manifestation of fracture in relations to the probable energy of the propagating crack and the precise surface energy, which requisites to be surpassed to initiate the propagation of cracks. The occurrence of surface defects, structural insertions or water all diminishes this critical energy value, facilitating crack propagation at lower stresses [Griffith,1920]. Nearly all-composite restorations are under recurring loading as protracted, as they withstand while being subjugated to masticatory loadings (118). In fact, resin composites do experience fracture strength degradation while defying fatigue scenarios (19). The flexural strength of composites can decrease up to 27% after being stressed under rotating fatigue (114). Likewise, dramatic strength degradations ranging from 32% up to 64% were witnessed for resin composite subjected to a flexural fatigue regimen of  $10^4$  cycles (122, 123). Similar strength degradation (37 up to 67%) were reported by Lohbauer *et al.* for resin composites after a fatigue challenge of  $10^5$  cycles (114).

The strength degradation over time is correlated to the material's susceptibility to SCG (19). The fatigue lifespan of the specimen is the amount of cycles of changeable stress and strain that a specimen can endure before failure occurs. The fatigue life for each specimen is different because it's reliant on the scale of the fluctuating stress, the specimen geometry and testing situations. The dynamic fatigue is one methodology, which relies on mathematical relationships among fracture endurance values attained at different constant non-zero stress



rates. Dynamic fatigue testing is favored over fracture-mechanic-based crack procreation tests because it yields more conformist lifetime appraisals, and the defects causing failure are more realistic. The fatigue test can be implemented by using a uni-axial or biaxial test with or without trifling flaws prompted by a sharp indenter.

Thus, the fatigue parameters  $n$  (stress corrosion susceptibility coefficient) is significant in expressing susceptibility against SCG and  $\sigma_{f0}$  (scaling parameter), an indication of the early strength of the material when subjected to mechanical loads. Both are reliant on the chemical environment and its bustle at the crack tip. A greater subcritical crack growth resistance or higher  $n$  value indicates slower strength degradation and higher enduring strength, consequently longer lifetime (124). Usually,  $n$  values ranging from 5 to 30 indicate a high susceptibility to strength degradation under corrosive environment over time. In the scientific literature, it has been exhibited that  $n$  values ranging from 7 to 34 for resin composites, 15 to 28 for feldspathic porcelains and glass-ceramics and 60 to 95 for high-density alumina (18) (122, 123, 125-129). Results of SCG parameters ( $n$  and  $\sigma_{f0}$ ) from different studies in implication to dental restorations are summarized in Table 2.2. It evidently displays the variation in the SCG parameters among different dental materials, thus echoing the importance of knowing these parameters of each different material in order to assess the strength degradation.

Table 2.2. Subcritical crack growth parameters of different dental restorative materials.  
(Rosa V *et al.*, 2008, Loubauer *et al* 2008, and Borba *et al* 2011)

Study	Year	Materials	Type	n	$\sigma_{f0}$ (Mpa)
Rosa V. <i>et al</i>	2008	Dental Porcelain	Control	24.1	58.1
			Ion Exchanged	36.7	127.9
Loubauer <i>et al</i>	2008	Glass Ceramic		19.16	
Borba <i>et al</i>	2011	Ceramics	Vita In-Ceram	76	880
			Vita In-Ceram Zirconia	54	408
			Veneering Porcelain Vita VM7	36	65.1
			Vita VM9	44	60.6

Dynamic fatigue test results, aid to formulate lifetime curves to predict the material's strength over time subjected to constant stress (e.g. 5 years). It implicates either lengthened term tests to measure time-to-failure under a static stress or the effect of subcritical behavior on the strength of specimens stressed at different rates, in what are known as 'dynamic' fatigue experiments (120). The assessment is performed using natural flaws; therefore, it will relate to the nature of distribution and size of the flaw population. Whereas in long crack experiments the statistical variation in data results from direct measuring errors (120).

A continuous application of mechanical and environmental loads eventually leads to progressive degradation and crack initiation and growth,

resulting in catastrophic failure of dental restorations. This procedure is further aided by pre-existing voids presented during material processing, imperfect interfaces, and residual stresses, causing resistance to crack initiation and growth an important consideration for a reliable assessment of dental restorations.

Unfortunately, clinical trials engaged in the long-term estimation of resin composite restorations provide rather seemingly to our understanding of their fracture behaviour. As periods for comprehensive observation are usually unavailable, incomplete observations often lead to premature interpretations, due to the dynamic behaviour of survival curves (129). Still one of the main reasons for restoration loss is fracture, due to mechanical fatigue degradation (115). Fatigue testing is the application of continuous loading to a test specimen in order to determine how it performs under repeated vibration or strain conditions. Clinically, an accumulation of the microstructure damage during mastication may induce a catastrophic failure. Therefore, fatigue is an aspect of clinical performance of restorations.

Thus, the mechanical tests and qualitative analysis can be close to clinical simulations of the oral environment and would be pivotal to assess the longevity of composite restorations as well due to flaw distribution and the initiation of the SCG. Henceforth, in contention to the “new class” that is the bulk-fill resin composites, this would be the pristine study to show the strength degradation and reliability over time under fatigue conditions. Furthermore, this would be vital in evaluating their service life *in-situ*.

## Chapter 3

# Aims and Hypothesis

---

### 3.1 Aims

The objective of this study was

To determine the Weibull ( $m$  and  $\sigma_0$ ) and Slow Crack Growth ( $n$  and  $\sigma_{f0}$ ) parameters of bulk-fill resin composite materials. In addition, the strength degradation over time was assessed for the materials tested, by the analysis of a strength-probability-time (SPT) diagram.

### 3.2 Hypothesis

The hypothesis to be tested is

Bulk-fill resin composites present Weibull and Slow crack growth (SCG) parameters comparable to the conventional resin composite tested.

# Chapter 4

## Materials and Methods

---

### 4.1 Resin Composite materials tested

The three bulk-fills and one conventional resin composite used in this study are listed below (Figure 4.1 to Figure 4.4), with their composition as shown in Table 4.1.



Figure 4.1. Tetric EvoCeram Bulk-fill resin composite - **TBF**



Figure 4.2. X-tra fil Bulk-fill resin composite - **XTR**



Figure 4.3. Filtek Bulk-fill resin composite (flowable) - **BFL**



Figure 4.4. Filtek Z250 (Conventional composite) – **Z250**

Table 4.1. Chemical composition of matrix, filler and filler content by weight (Wt%) and volume (Vol%) of resin composites used as by manufacturer

Resin based composites	Group	Resin matrix	Filler	Filler Wt%/Vol%
Tetric EvoCeram Bulk fill nanohybrid (Vivadent, USA, batch S14902)	TBF	Bis-GMA, UDMA, Bis-EMA	Ba-Al-Si glass, prepolymer filler (monomer, glass filler and ytterbium fluoride), spherical mixed oxide	81/61
x-tra fil hybrid (VOCO, USA, batch 1325395)	XTR	Bis-GMA, UDMA, TEGDMA	N/A	86/70
Filtek Bulk fill Flowable (3M ESPE, USA, batch N504062)	BFL	Bis-GMA, UDMA, Bis-EMA, Procrylat resins	Zirconia/silica, ytterbium trifluoride	64/42
Filtek Z250 (3M ESPE, USA, batch 1370A3)	Z250	Bis-GMA, UDMA, Bis-EMA	Zirconia/silica	82/60

Abbreviations: Bis-GMA (Bisphenol A diglycidyl ether dimethacrylate), Bis-EMA (Bisphenol A polyethylene glycol diether dimethacrylate), UDMA (urethane dimethacrylate), TEGDMA (triethylene glycol dimethacrylate), N/A (Not Available)

## 4.2 Specimen fabrication

Disk-shaped specimens (12 mm in diameter and  $1.0 \pm 0.1$  mm thick) were prepared by inserting the uncured composites in a stainless steel split mold. The top surface was covered with a Mylar strip. A glass slide was placed over the mold and manual pressure was applied to extrude excess material. The glass slide was removed and the material was photoactivated for 20s as specified by the manufacturer at  $1200 \text{ mW/cm}^2$  (Elitedent Q-4, Elitedent Enterprise Inc, USA). The tip of the curing light was kept 2 mm from the composite by a spacer to standardize curing distance, cured at single spot. The specimens were subsequently removed from the mold. The specimens obtained were not polished. Specimens' dimensions were recorded with a

digital caliper (model CD-6, Serial no. 7144876, Mitutoyo Corp., Japan). and stored in distilled water at 37 °C for 24 hours prior to testing. For each material tested 75 specimens were fabricated.

### **4.3 Degree of conversion**

The degree of conversion (DOC) was assessed to confirm the efficacy of the polymerization method. Five specimens were dry stored for 24 hours at 37 °C and the FT-IR spectrum was measured at the bottom of the specimens in mid-IR region (IFS66v/S, Bruker, USA) equipped with universal ATR sampling accessory (MIRacle, PIKE, USA) under the following conditions: 4 cm<sup>-1</sup> resolution and 138 scans per spectrum (Figure 4.5). DOC was obtained by measuring the difference in the ratio of the absorbance strength of the vinyl peak at 1638 cm<sup>-1</sup> and a reference peak at 1608 cm<sup>-1</sup> corresponding to aromatic absorption before and after photoactivation according to previously reported (8).



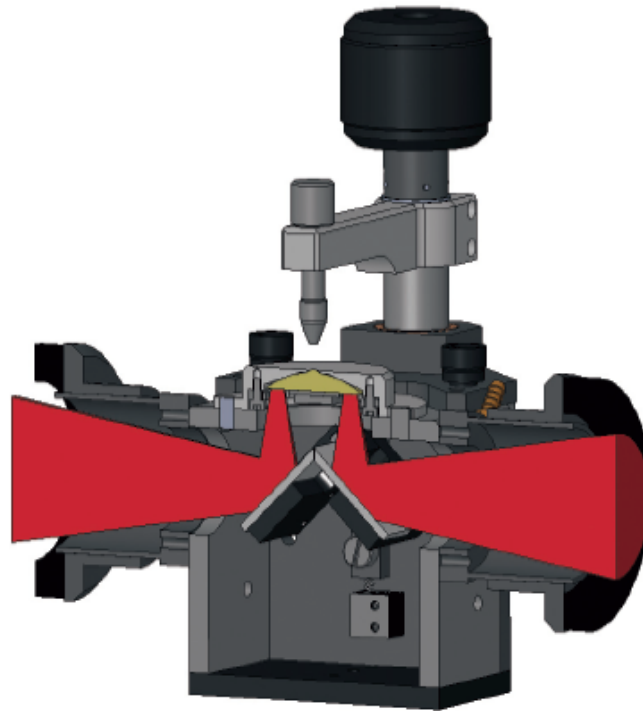


Figure 4.5. MIRacle (PIKE, USA) – High Throughput and Efficient Optical Design

#### **4.4 Dynamic fatigue test**

The biaxial flexural strength of 70 specimens of each material were tested under distilled water (37 °C) with a piston-on-three balls device using a universal testing machine (Model 5948 MicroTester, Instron, USA) (130) as shown in Figures 4.6 - 4.8

The experiment was performed in a custom-made chamber filled with distilled water and the temperature was controlled at 37°C by a custom-made tank. Water from the chamber streamed into a reservoir tank where in the heater was maintained and circulated warm water back into the test chamber. Water circulation was constant

during the experiment in order to maintain the temperature at 37°C ( $\pm 1^\circ\text{C}$ ). Each specimen was placed centrally on the three balls, with the surface away from the light facing down (Figure 4.6) The tip of the piston was aligned perpendicularly to the centre of the disc at a crosshead speed of 0.5 mm/min until failure occurred (Figure 4.7 and 4.8)

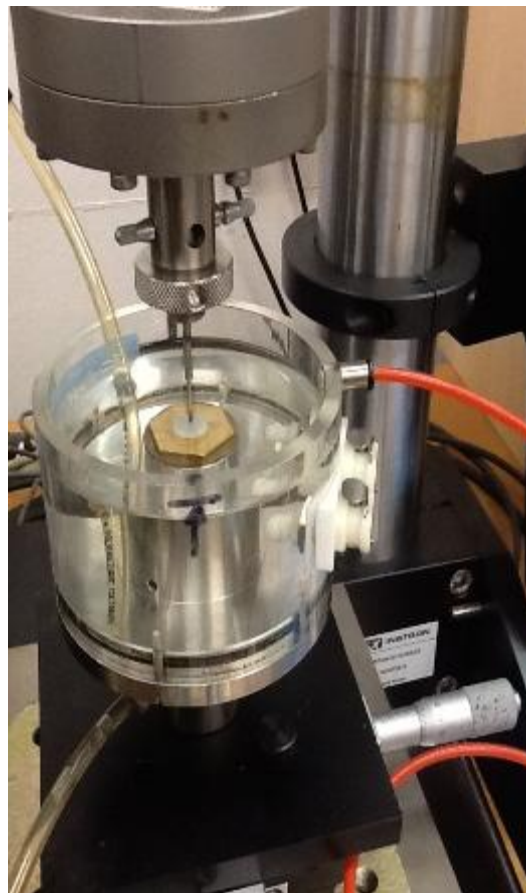


Figure 4.6. Biaxial flexure strength test set up

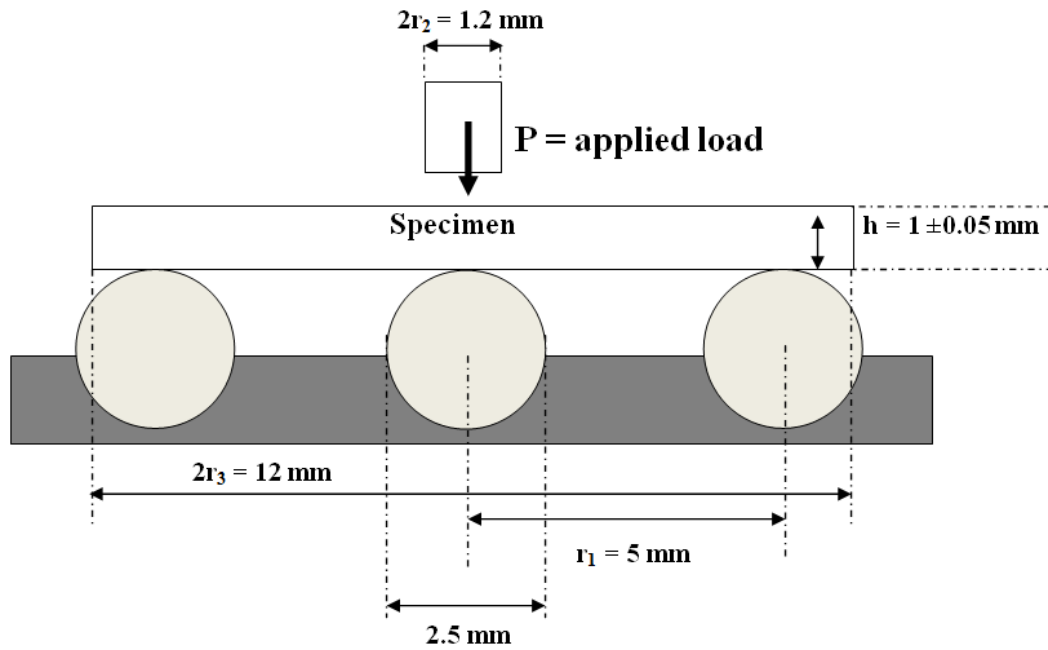


Figure 4.7. Axial view of schematic drawing of piston-on-three-balls setting for biaxial flexural test (Adapted from Ornaghi *et al.*, 2012, Pick *et al.*, 2010).

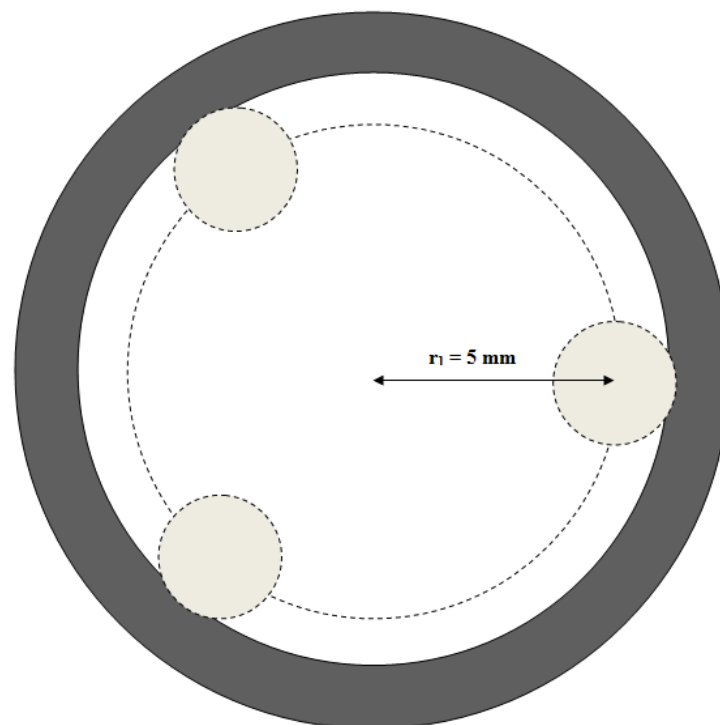


Figure 4.8. Coronal view of schematic drawing of piston-on-three-balls setting for biaxial flexural test (Adapted from Ornaghi *et al.*, 2012, Pick *et al.*, 2010).

The SCG parameters  $n$  (subcritical crack growth susceptibility coefficient) and  $\sigma_{f0}$  (scaling parameter) were obtained by the dynamic fatigue method which relies on mathematical relationships among fracture resistance values obtained at different constant non-zero stress rates (18, 19, 116). The higher the  $n$  value calculated, the lower susceptibility to SCG. Ten specimens were tested in each of the stress rates ( $10^{-2}$ ,  $10^{-1}$ , 1,  $10^1$  and  $10^2$  MPa/s) with the exception of 1 MPa/s, for which thirty specimens were tested to perform Weibull statistics (123). No pre-load was used at all stress rates.

The biaxial flexural strength ( $\sigma_f$ ) was obtained according to ISO 6872 (131) as previously described by Ornaghi *et al* (19):

$$\sigma_f = \frac{-0.2387P(X-Y)}{b^2} \quad \text{Equation 4.1.}$$

$$X = (1 + \nu) \ln \left( \frac{r_2}{r_3} \right)^2 + \left[ \frac{1-\nu}{2} \right] \left( \frac{r_2}{r_3} \right)^2 \quad \text{Equation 4.2.}$$

$$Y = (1 + \nu) \left[ 1 + \ln \left( \frac{r_1}{r_3} \right)^2 \right] + (1 - \nu) \left( \frac{r_1}{r_3} \right)^2 \quad \text{Equation 4.3.}$$

where  $P$  is the failure load (in N),  $b$  is the thickness of the specimen (in mm),  $\nu$  is the Poisson's ratio ( $\nu = 0.30$  for all composites (132)),  $r_1$  is the radius of the support ball circle (5 mm),  $r_2$  is the radius of loaded area (0.6 mm) and  $r_3$  is the radius of the specimen (6 mm) (Figure 4.8.). The SCG parameters ( $n$  and  $\sigma_{f0}$ ) were calculated according to equation 4.4 where  $\dot{\sigma}$  is the stress rate.

$$\log \sigma_f = \left( \frac{1}{n+1} \right) \log \dot{\sigma} + \log \sigma_{f0} \quad \text{Equation 4.4.}$$

The dynamic fatigue curves were obtained by the correlation between  $\sigma_f$  and loading rate. By plotting the correlation between  $\sigma_f$  and time for failure in logarithmic scale, it was possible to determine the fracture strength corresponding to time to failure at 1 day ( $\sigma_{1d}$ ), 1 year ( $\sigma_{1y}$ ) and 5 years ( $\sigma_{5y}$ ) of each composite tested.

#### 4.5 Weibull analysis and Strength-probability-time diagram

Weibull analysis is used to identify the reliability and probability of fracture of brittle materials. The strength results of specimens tested at 1 MPa/s ( $n = 30$ ) were integrated to the two-parameter Weibull distribution. The Weibull modulus ( $m$ ) and the characteristic strength ( $\sigma_0$ ), which corresponds to the strength at the failure probability of 63.2%, were calculated using equation 4.5 where  $P_f$  is the fracture probability:

$$P_f = 1 - \exp \left[ - \left( \frac{\sigma_f}{\sigma_0} \right)^m \right] \quad \text{Equation 4.5.}$$

The parameters  $m$  and  $\sigma_0$ , in addition to their 95% confidence interval were obtained using the maximum likelihood method, according to ASTM C 1239 (133)

The strength-probability-time (SPT) diagrams were obtained by merging the Weibull parameters to the results obtained in the dynamic fatigue test (134). The SPT diagram allows the prediction of fracture stress under constant stress for different probability levels at a given period of time.

Statistical analysis was performed using ANOVA and multiple comparisons

were performed using Bonferroni's post hoc test at a pre-set significance level of 5%. Statistics were performed for the comparison of biaxial flexure strength amongst stress rate for each material respectively and for the degree of conversion. The fatigue parameters were analyzed according to the guidelines presented in ASTM C 1368-00 (130) .

# Chapter 5

## Results

---

### 5.1 Dynamic fatigue test

The biaxial flexure strengths shown as a function of stress rate is displayed in Figure 5.1 with the mean values at every stress rate for each material tested in Table 5.1. It can be observed that there is an increase in the fracture strength with each increased stress rate for all the composites tested. Z250 presents with the highest fracture strength at all stress rates (Table 5.1), BFL and TBF show similar fracture strength but lower than XTR (Table 5.1 and Figure 5.1). Statistical difference is shown in Table 5.1 among the different stress rates for each material.

Table 5.1. Biaxial flexural strength (in MPa) and standard deviation (in parenthesis) of all the materials tested.

Stress rate (MPa/s)	Fracture strength			
	TBF	BFL	XTR	Z250
100	121.76 (8.3) <sup>A</sup>	124.81 (21.2) <sup>A</sup>	177.07 (12.4) <sup>A</sup>	189.43 (41.3) <sup>A</sup>
10	120.11 (9.3) <sup>A</sup>	131.75 (17.2) <sup>A</sup>	147.65 (26.1) <sup>B</sup>	181.51 (43.5) <sup>A</sup>
1	114.57 (51.4) <sup>A</sup>	115.83 (15.5) <sup>AB</sup>	141.58 (15.7) <sup>BC</sup>	169.02 (20.9) <sup>A</sup>
0.1	103.78 (10.7) <sup>AB</sup>	120.91 (15.6) <sup>A</sup>	126.39 (6.9) <sup>DCB</sup>	133.71 (36.3) <sup>B</sup>
0.01	85.69 (8.6) <sup>B</sup>	95.53 (15.6) <sup>B</sup>	108.90 (7.5) <sup>D</sup>	114.94 (22.8) <sup>B</sup>

---

Same letters in the uppercase indicate statistically similar values compared in the columns.

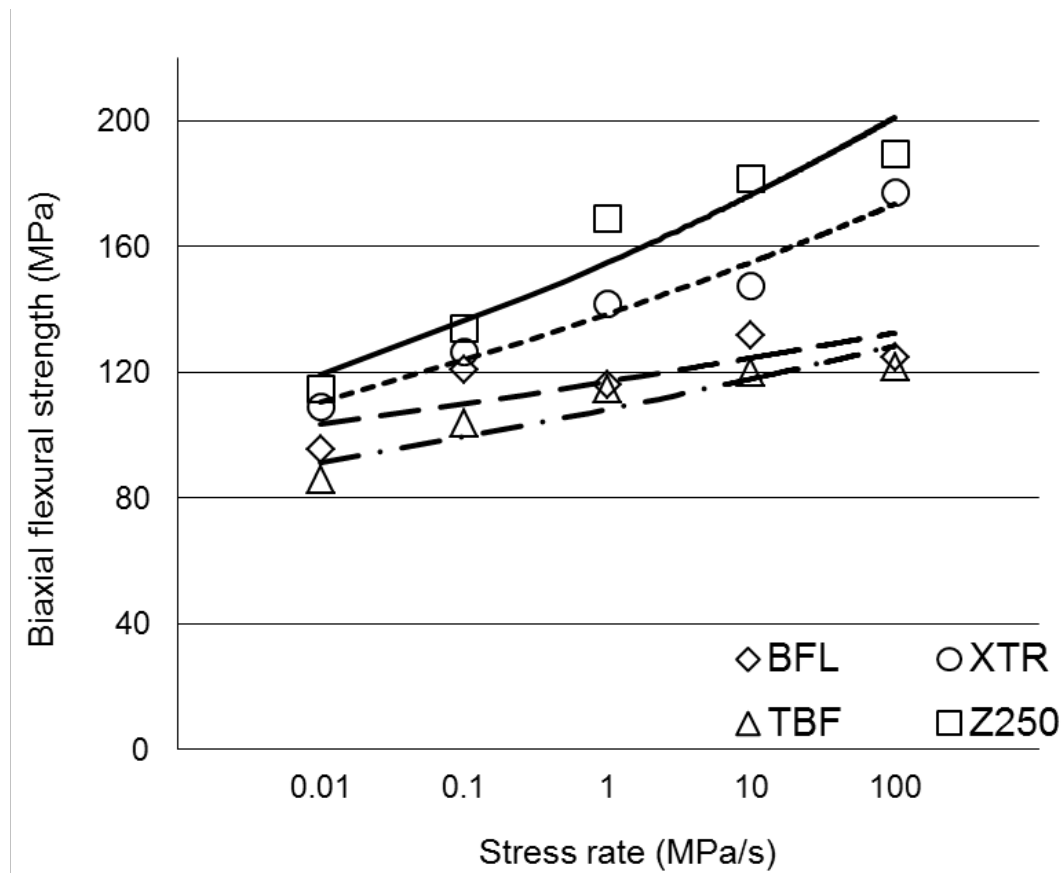


Figure 5.1. Flexural strength as a function of stress rate of the materials tested.

Alongside, Figure 5.2 displays the time taken (in min) to fracture each specimen at given stress rates respectively. The longest time taken to fracture each specimen is clearly seen in the slowest stress rate of 0.01 MPa/s. TBF, BFL, XTR and Z250 taking 142.82, 159.22, 181.50 and 191.44 min to fracture each specimen. In higher stress rates of 10 and 100 MPa/s the time taken to fracture was negligible. There was a significant statistical difference amongst all the material tested except between XTR and Z250 at 0.01 MPa/s stress rate (Figure 5.2).



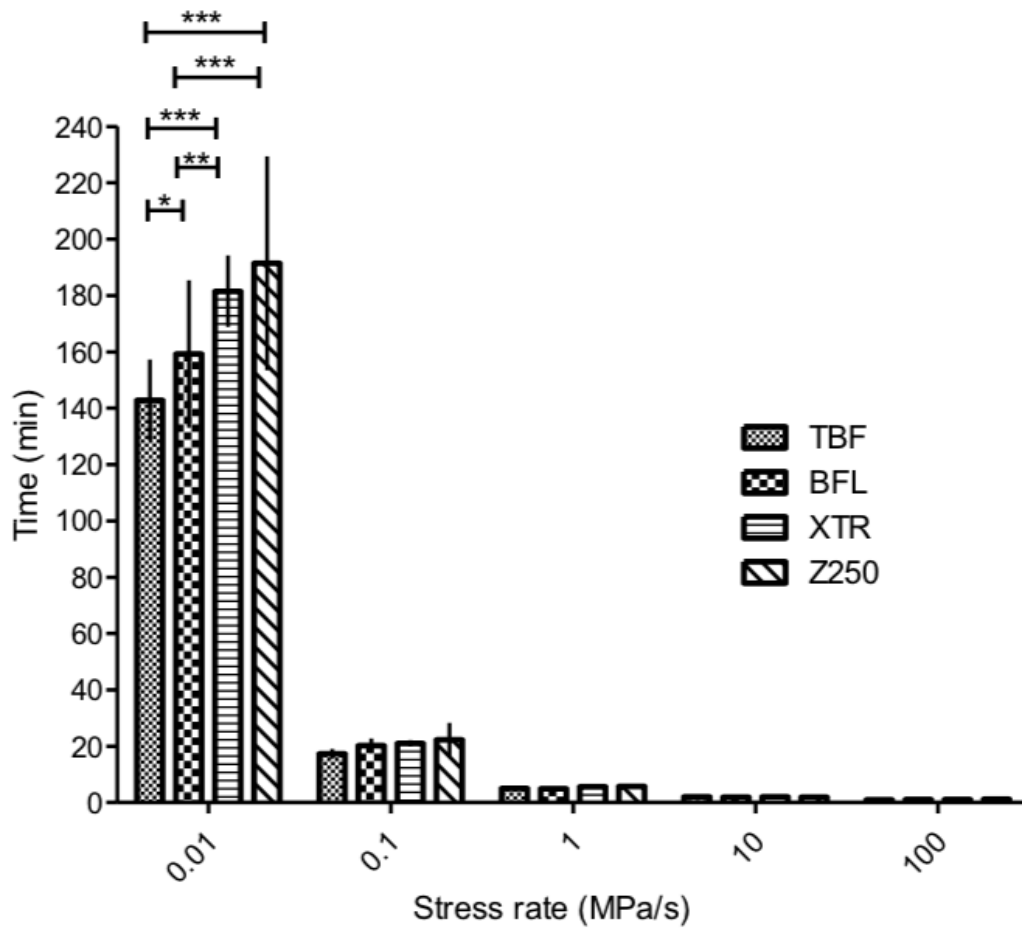


Figure 5.2. Time taken to fracture each specimen at given stress rates for all materials tested respectively. [(\*) indicates  $p < 0.05$ , (\*\*) indicates  $p < 0.01$ , (\*\*\*) indicates  $p < 0.001$ ]

Table 5.2 exhibits the DOC and SCG parameters ( $n$  and  $\sigma_{f0}$ ) for the materials tested. The DOC values for all materials were statistically similar, around 60% ( $p=0.8841$ ). Within the range XTR presented the highest DOC where as Z250 presented the lowest (Table 5.2).

While BFL presented the highest  $n$  value (40.1) and an interim  $\sigma_{f0}$  value (114.56) and Z250 showed lowest  $n$  value (16) and highest  $\sigma_{f0}$  values (157.02) respectively. The  $n$  value for BFL was the highest obtained, followed by TBF (25.5). XTR presented  $n$  values (16.6) similar to Z250. However the  $\sigma_{f0}$  value for XTR and TBF were 140.81 and 110.90 respectively.

Table 5.2. Degree of conversion after 24 hours (DOC),  $n$  (subcritical crack growth susceptibility coefficient) and  $\sigma_{f0}$  (scaling parameter), with respective standard deviations in parenthesis

	TBF	BFL	XTR	Z250
DOC	57.6 (12.0) <sup>a</sup>	64.6 (3.6) <sup>a</sup>	67.1 (5.9) <sup>a</sup>	55.3 (7.7) <sup>a</sup>
$n$	25.5 (3.5)	40.1 (12.2)	16.6 (1.5)	16.0 (2.6)
$\sigma_{f0}$	110.90 (0.01)	114.56 (0.02)	140.81 (0.01)	157.02 (0.03)

The logarithmic transformation of the time to failure and fracture resistance provided the lifetime curve (Figure 5.3) with the correlating derived fracture stresses for 1 day, 1 year and 5 years. Values of which are shown in Table 5.3. It was conceivable that higher the  $n$  value, lower the slope, deducing a lower susceptibility to SCG and eventually lower strength degradation over time. Thus, the difference in the strength decadence can be observed in Figure 5.3 in which the curve corresponding to Z250 ( $n=16$ ) shows a steeper slope whereas the slope for BFL

(n=40.1) is the least. Moreover also observed here, is that even though BFL has lower initial strength (Table 5.2) it will degrade less over time (Table 5.3). Strength degradation calculated after 5 years for BFL was 13%, followed by TBF (26%), Z250 (32%) and XTR (35%).

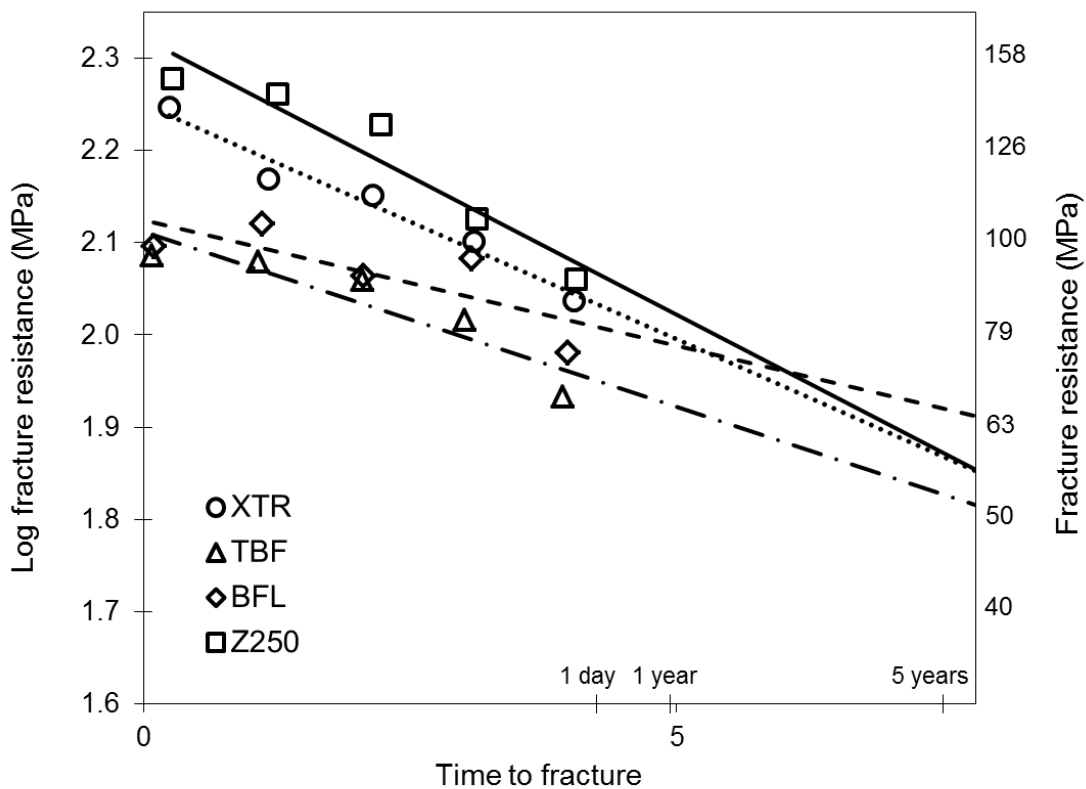


Figure 5.3. Lifetime curve the log of flexural strength (in MPa) to the log of time of fracture. The time axis is labeled for 1 day, 1 year and 5 years.

Table 5.3. Fracture stresses (MPa) estimated for 1 day ( $\sigma_{1d}$ ), 1 year ( $\sigma_{1y}$ ) and 5 years ( $\sigma_{5y}$ )

	TBF	BFL	XTR	Z250
$\sigma_{1d}$	85.9	98.4	101.3	111.1
$\sigma_{1y}$	69.3	85.3	75.9	80.9
$\sigma_{5y}$	63.4	80.7	67.9	71.5

## 5.2 Weibull analysis and strength-probability-time

The Weibull parameters and plots are presented in Table 5.4 and Figure 5.4, respectively. Table 5.4 shows the  $m$  and  $\sigma_0$  values for all composites. Where  $m$  expresses the materials reliability based on its flaw distribution. There was no significant difference in the  $m$  value obtained for all materials as the 95% confidence intervals overlap. Statistically, the  $m$  values of all the materials tested are similar.

Figure 5.4 represents individual graphs with the Weibull plot for each of the materials tested respectively. The Weibull plot shown for all the materials respectively with the 95% confidence interval of  $m$  and  $\sigma_0$ , where it is possible to note a higher variability of strength data in Z250. For  $\sigma_0$ , Z250 and XTR were different and significantly higher than TBF and BFL. The latter were similar as the confidence intervals overlap.

The 95% confidence interval in all the bulk-fill resin composites for  $m$  appear to be in the similar range as compared to the conventional composite (Z250). Whereas the 95% confidence interval for  $\sigma_0$  shows the lowest value for Z250 (169.5 MPa) is higher than the highest value among the bulk-fill resin composites tested (154.8 MPa) (Table 5.4). The characteristic strength of Z250 is much higher on comparison to BFL. It can be inferred that the characteristic strength of Z250 is high by 31% to that of BFL. The lowest value of the strength of Z250 is 9% higher to the highest value of XTR (Table 5.4).

Table 5.4. Weibull modulus ( $m$ ), characteristic strength ( $\sigma_0$ ) and 95% confidence intervals in parenthesis.

	TBF	BFL	XTR	Z250
$m$	9.7 (6.8 – 12.5)	8.9 (6.5 – 12.1)	9.7 (7.1 – 13.0)	8.6 (6.3 – 11.6)
$\sigma_0$ (MPa)	120.3 (115.1 – 125.7)	122.4 (116.7 – 127.9)	148.4 (142.2 – 154.8)	177.8 (169.5 – 186.4)

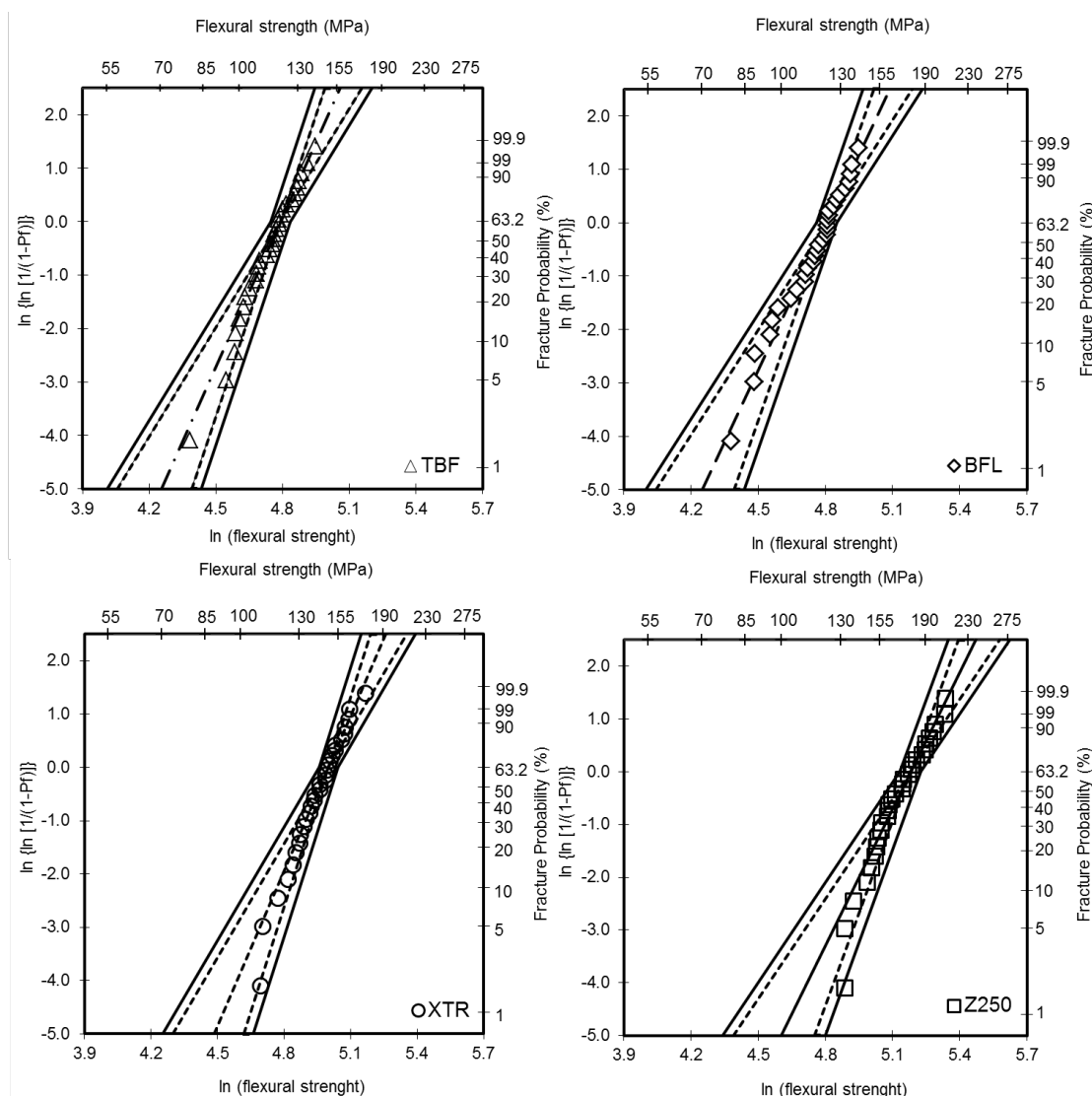


Figure 5.4. Weibull plot of the flexural strength test for the tested group of materials. Dashed lines represent the 95% confidence interval of Weibull modulus and straight lines represent the 95% confidence interval of the Weibull modulus combined with characteristic strength.

The SPT diagrams for 1 and 5 years were obtained from the interpolation of dynamic fatigue and Weibull data and are presented in Figure 5.5. This graph also gives us the perspective of what would be the stress to fracture 5% of the specimens after 5 years. The fracture stresses (in MPa) corresponding to the 5% of failure probability is seen in Table 5.5. Strength degradation overtime was higher for Z250 and XTR as compared to TBF and BFL. Z250 had the highest strength for all fracture probabilities after 1 year and BFL after 5 years simulations. Though the degradation for BFL after 1 year was high (62.80 MPa) , after 5 years the predicted failure stress for the 5% probability decreased by only 18% (50.90 MPa) to that of 25%,32% and 36% of TEC, XTR and Z250 respectively (Table 5.5).

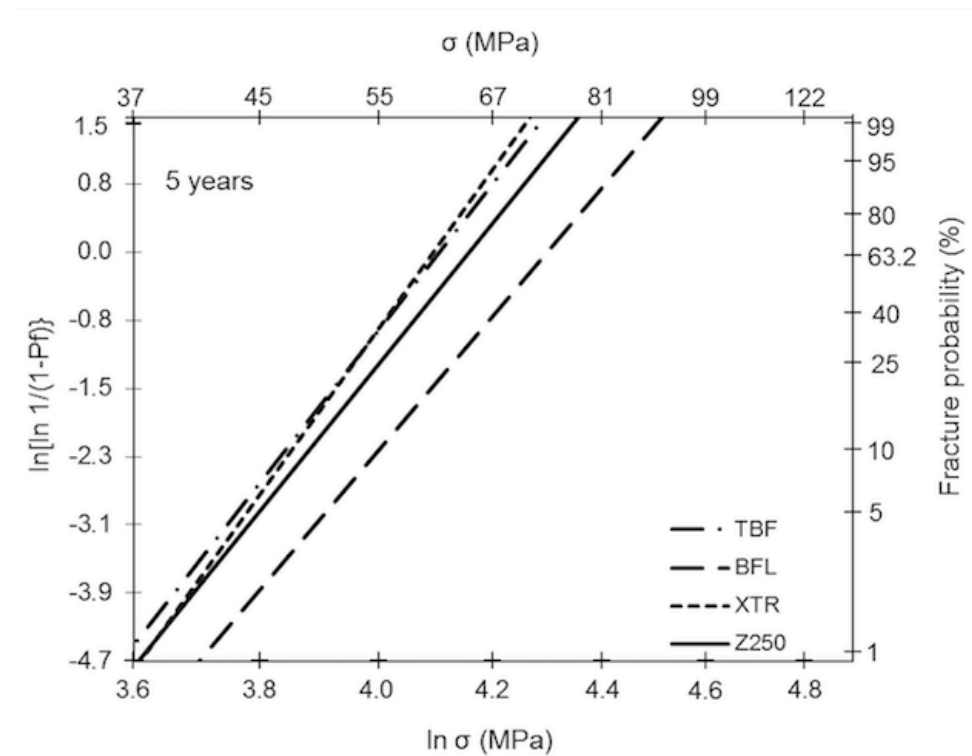
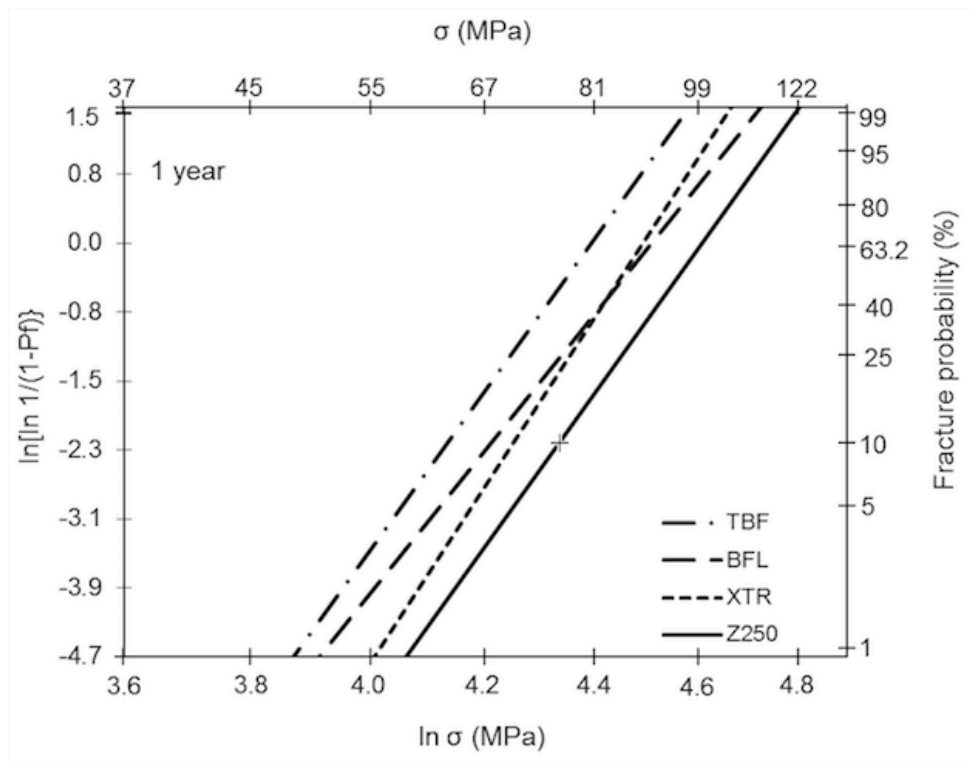


Figure 5.5. SPT diagram of all the composites tested. The lines correspond to the fracture stresses ( $\sigma_a$ ) for the time of failure of 1 year and 5 years.



Table 5.5. Reliability probability over time - Strength at more clinically relevant failure probability of 5% at different times for all the composite materials

Time	Strength (Mpa)			
	TBF	BFL	XTR	Z250
1 year	55.55	62.80	66.02	72.24
5 years	43.81	50.90	44.70	46.06

## Chapter 6

# Discussion

---

The hypothesis of this study was partially accepted as bulk-fill resin composites present similar Weibull modulus than conventional resin composite. On the other hand, the fracture strength and susceptibility to slow crack growth was dependent on the material composition. Bulk-fill resin composite presented fatigue resistance over time higher to the conventional composite tested.

The development of SCG phenomenon is determined by the stress value growing in the material, which sequentially depends on stress rates applied during the test. In Table 5.1, it is observed that  $\sigma_f$  is directly associated to the stress rates for all composites. As the stress rates increase the flexure strength increases.

Interestingly, with the increase in the stress rates the time taken to fracture each specimen decreased. It is seen Figure 5.2, that maximum time to fracture each specimen was at the stress rate of 0.01 MPa/s. Z250 and XTR specimens took the maximum time to fracture at 3 hours, followed by BFL and TBF which took a little over 2 hours at this stress rate. Whereas, for the other stress rates of 0.1, 1, 10 and 100 MPa/s the time ranges from 1 min. to 20 min. With 50 specimens tested for each material, to obtain SCG parameters it is very time consuming. As shown in Table 5.1, Z250 presented an average fracture strength of 114 MPa at 0.01 MPa/s. The time accounted to test each sample was 3 hours. Considering a sample size of 10

specimens per stress rate for each material, the time taken to test the specimens in this stress rate only for Z250 alone is about 30 hours. Thus the time required to perform this assay may be one of the reasons why there is a lack in literature about information of fatigue behaviour of materials, leading to the popularization of tests that reflect flexural strength for fast fracture only.

SCG can occur in dental ceramics and resin composites as a result of the blend of subcritical tensile stresses and a corrosive environment (18-20, 135). To persist the circumstances in the oral environment, resin composites must impart high fracture strength at the onset of SCG ( $\sigma_0$ ) and low strength degradation ( $n$ ) over time (19). The dynamic fatigue method is used to determine these SCG parameters in brittle restorative materials such as ceramics and resin composites (18-20, 125, 136). Dynamic fatigue testing yields more conservative lifetime estimates, and the flaws causing failure are more realistic. Despite that, the viscoelastic relaxation of resin composites is a cause of concern while estimating fatigue behaviors based on SCG phenomena (19).

As water sorption of resin composites over 24 hours is almost 50% of that after 180 days (137), it can be expected that just after the placement of the restoration, the near surface flaws in composite may be exposed to corrosive environments. Once the fatigue crack instructs in resin composites, the dissemination follows a stable sub-critical growth mode, indicating that the failure process is primarily driven by the stress concentration at the tip of the crack (138). Additionally, fractographic analyses of specimens tested under dynamic fatigue revealed the presence of crack with semi-elliptical shape, hackle lines and mirror zone (19) characteristic of brittle failure (18, 20, 139). The SCG depends on the stress level developed in the material, which in

turn depends on the stress rate used during the dynamic fatigue test, and as anticipated, the lower the stress rates applied, the lower the flexural strength (Figure 5.1). Values of  $n$  ranging from 5 to 30 indicate a high susceptibility to SCG. Hence, all materials tested were susceptible to stress corrosion with the exception of BFL. The high susceptibility of resin composites to fatigue has also been previously shown by other studies (104, 107, 114).

In fact, high values of flexural strength and fracture toughness may not directly translate into fatigue resistance (123). Strength degradation is presented in Figure 5.3. Among the materials tested, Z250 is expected to degrade more over time as it had the lowest  $n$  value, even though it had higher initial strength ( $\sigma_{f0}$ ) than BFL. Such difference in strength decadence can be observed in Figure 5.1 in the curve corresponding to the Z250 shows a steeper slope. After 5 years, the strength degradation was 59% for Z250 and 18% for BFL (Table 5.3). This was also seen in TBF, in spite of a low  $\sigma_{f0}$  of 110.9, its high  $n$  value = 25.5 resulted in estimated strength decadence after 5 years of only 26%. Thus, signifying higher the  $n$  value lower will be the slope. This in turn is relevant clinically as an outlier to the strength degradation of the material as they are subjected to fatigue in the oral scenario as soon as they are placed in the oral cavity.

As the DOC was similar for all materials, the lower strength degradation of BFL over Z250 may be an effect of the widespread granulometric distribution of BFL (0.01 to 5  $\mu\text{m}$ ) as compared to Z250 (0.01 to 3.5  $\mu\text{m}$ ) (66). The filler type and loading has been associated to affect crack propagation, specifically the incorporation of fillers to improve the loading and packing efficiency, enabling an rise in volume fraction of the filler (140). This may ensue in an amplified likelihood for crack

deflection and less strength degradation over time (138). This can translate into a better polymerized matrix, that secures a meshwork between the large and the small particles, lessening water uptake and subsequently, inhibiting crack propagation under corrosive environment. However, the compositions of materials shown in Table 4.1 was not obtained by independent researchers. Thus, prudence is needed when extrapolating conclusions from data provided by manufacturers only (123).

In Weibull analysis, the distribution of the flaws is taken into consideration to give the reliable strength of the material. (141, 142). Here, the Weibull modulus ( $m$ ) was in the same range for all materials tested and varied from 8.6 up to 9.7 (Table 5.4). Thereby predicting similar reliability. However, although the  $m$  value was similar across the materials tested,  $\sigma_0$  was at least 16% higher for Z250 as compared to the bulk fill resin composites. Moreover, where XTR presented  $n$  value similar to Z250, both BFL and TBF had a  $n$  value higher to that of Z250.

Even though the value of  $m$  for some bulk-fill composites can be as high as 21.6 or 26.7, values for TBF and BFL found in this study were similar to those reported previously (7). Though the materials present similar reliability, they differ in terms of strength. The  $\sigma_0$  for BFL and TBF are similar and approximately 30% lower than that of Z250. Considering the 95% confidence interval for  $\sigma_0$ , the lowest value of Z250 (169.5 MPa) was only 8% higher than the highest value obtained for XTR (154.8 MPa). We also verified the strength at the more clinically relevant failure probability of 5% as  $\sigma_0$  is the stress level at which 63.2% of specimens fail. Here, Z250 showed the highest strength (126 MPa) when related to XTR (109 MPa), BFL and TBF (~88 MPa). The performance of the latter composites may be explained by their lower filler volumes in comparison to XTR and Z250 (Table 4.1). Increased

filler volumes have been associated with increased flexural strength and flexural modulus (143). However, there are other variable factors that do effect the performance of the materials that need to be further unvestigated.

Thus, as Weibull analysis integrates the failure probability ( $P_f$ ) of a material analogous of the stress values ( $\sigma_f$ ), emerging closer to explain the range of defects in a specimen. By combining the results of a time-dependent analysis with the Weibull analysis it is possible to build or formulate simulations which estimates the material's fracture strength for a given failure probability over its lifetime (3, 18, 19). This data is shown in a strength–probability–time (SPT) diagram (125). Such diagram is commonly used to predict the maximum stress for dental ceramics at which the material should survive for both a given time span and percentage probability of failure (18, 141). In the clinic, one of the main reasons for catastrophic failures in composite restoration is bulk fractures, therefore to be able to predict the strength degradation with the reliabitily ober time for a given material would be critical in-situ.

The SPT diagrams for 1 and 5 years are depicted in Figure 5.5. After one year, Z250 dictates a stress of 72 MPa for failure, followed by XTR (66 MPa), BFL (62 MPa) and TBF (59 MPa) considering a 5% probability of failure. However, for TBF and BFL, the degradation on strength occured at a slower rate. Thus, BFL presents fracture strength of 51 MPa while the other materials range from 44 to 46 Mpa for the same failure probability after 5 years. After 5 years the predicted failure stress for 5% probability decreased by 18% for BFL, 25% for TEC, 32% for XTR and 36% Z250 respectively (Table 5.5). Thus it can be clearly seen that the fatigue degradation over time for BFL is double to that of Z250. In order to deduce these results in clinical practice we take into consideration the mean applied stress in each chewing cycle in

the molar region , which is approximately 28 MPa (141). It is possible to note that the fracture stresses for 5 years simulations (at 5% fracture probability) are much higher , infact double of the stress of 28 MPa mentioned above.

Within the limitaton of our study we observed that with the specimens produced with 1mm thickness bulk-fill resin composites with respect to fatigue degradation behave comparable or higher to the conventional composite. However, to know if these materials would behave the same when used in 4mm thickness as the degree of conversion could decrease, further in-vitro studies shall be progressed in compliance with the clinical scenario.

## Chapter 7

# Conclusions

---

The studied resin composites presented similar Weibull modulus. The fracture strength and resistance to slow crack growth were influenced by the material composition. Bulk-fill composites (BFL and TBF) presented higher stress corrosion coefficient ( $n$ ) in comparison to the conventional composite tested. In the SPT diagram, BFL presented the least degradation for all fracture probabilities after 5 years. Nevertheless, for a fracture probability of 5% at this time point, all the materials tested demand higher fracture stresses than the mean applied stress in the molar region in clinical setting. Thus, this evaluation of the bulk-fill could be imperative in controlling catastrophic fatigue failures, which is of critical importance clinically.



# References

1. Blank JT, Latta M. Composite resin layering and placement techniques: case presentation and scientific evaluation. *Pract Proced Aesthet Dent*. 2005;17:385-90; quiz 92.
2. Sarrett DC. Clinical challenges and the relevance of materials testing for posterior composite restorations. *Dent Mater*. 2005;21:9-20.
3. El-Safty S, Silikas N, Watts DC. Creep deformation of restorative resin-composites intended for bulk-fill placement. *Dent Mater*. 2012;28:928-35.
4. Leprince JG, Palin WM, Vanacker J, Sabbagh J, Devaux J, Leloup G. Physico-mechanical characteristics of commercially available bulk-fill composites. *J Dent*. 2014;42:993-1000.
5. Alshali RZ, Silikas N, Satterthwaite JD. Degree of conversion of bulk-fill compared to conventional resin-composites at two time intervals. *Dent Mater*. 2013;29:e213-7.
6. Par M, Gamulin O, Marovic D, Klaric E, Tarle Z. Raman spectroscopic assessment of degree of conversion of bulk-fill resin composites--changes at 24 hours post cure. *Oper Dent*. 2015;40:E92-101.
7. Ilie N, Bucuta S, Draenert M. Bulk-fill resin-based composites: an in vitro assessment of their mechanical performance. *Oper Dent*. 2013;38:618-25.

8. Garcia D, Yaman P, Dennison J, Neiva G. Polymerization shrinkage and depth of cure of bulk fill flowable composite resins. *Oper Dent.* 2014;39:441-8.
9. Roggendorf MJ, Kramer N, Appelt A, Naumann M, Frankenberger R. Marginal quality of flowable 4-mm base vs. conventionally layered resin composite. *J Dent.* 2011;39:643-7.
10. Moorthy A, Hogg CH, Dowling AH, Grufferty BF, Benetti AR, Fleming GJ. Cuspal deflection and microleakage in premolar teeth restored with bulk-fill flowable resin-based composite base materials. *J Dent.* 2012;40:500-5.
11. Agarwal RS, Hiremath H, Agarwal J, Garg A. Evaluation of cervical marginal and internal adaptation using newer bulk fill composites: An in vitro study. *J Conserv Dent.* 2015;18:56-61.
12. Benetti AR, Havndrup-Pedersen C, Honore D, Pedersen MK, Pallesen U. Bulk-fill resin composites: polymerization contraction, depth of cure, and gap formation. *Oper Dent.* 2015;40:190-200.
13. El-Safty S, Silikas N, Akhtar R, Watts DC. Nanoindentation creep versus bulk compressive creep of dental resin-composites. *Dent Mater.* 2012;28:1171-82.
14. Kelly JR. Perspectives on strength. *Dent Mater.* 1995;11:103-10.
15. Czasch P, Ilie N. In vitro comparison of mechanical properties and degree of cure of bulk fill composites. *Clin Oral Investig.* 2013;17:227-35.
16. El-Safty S, Akhtar R, Silikas N, Watts DC. Nanomechanical properties of dental resin-composites. *Dent Mater.* 2012;28:1292-300.

17. McCabe JF, Carrick TE. A statistical approach to the mechanical testing of dental materials. *Dent Mater.* 1986;2:139-42.
  
18. Rosa V, Yoshimura HN, Pinto MM, Fredericci C, Cesar PF. Effect of ion exchange on strength and slow crack growth of a dental porcelain. *Dent Mater.* 2009;25:736-43.
  
19. Ornaghi BP, Meier MM, Rosa V, Cesar PF, Lohbauer U, Braga RR. Subcritical crack growth and in vitro lifetime prediction of resin composites with different filler distributions. *Dent Mater.* 2012;28:985-95.
  
20. Pinto MM, Cesar PF, Rosa V, Yoshimura HN. Influence of pH on slow crack growth of dental porcelains. *Dent Mater.* 2008;24:814-23.
  
21. Palin WM, Fleming GJ, Burke FJ, Marquis PM, Randall RC. The influence of short and medium-term water immersion on the hydrolytic stability of novel low-shrink dental composites. *Dent Mater.* 2005;21:852-63.
  
22. Ferracane JL. Hygroscopic and hydrolytic effects in dental polymer networks. *Dent Mater.* 2006;22:211-22.
  
23. Freund M, Munksgaard EC. Enzymatic degradation of BISGMA/TEGDMA-polymers causing decreased microhardness and greater wear in vitro. *Scand J Dent Res.* 1990;98:351-5.
  
24. Yap AU, Lee HK, Sabapathy R. Release of methacrylic acid from dental composites. *Dent Mater.* 2000;16:172-9.

25. Ferracane JL, Marker VA. Solvent degradation and reduced fracture toughness in aged composites. *J Dent Res.* 1992;71:13-9.
  
26. Yap AU, Chew CL, Ong LF, Teoh SH. Environmental damage and occlusal contact area wear of composite restoratives. *J Oral Rehabil.* 2002;29:87-97.
  
27. Thompson GA. Determining the slow crack growth parameter and Weibull two-parameter estimates of bilaminate disks by constant displacement-rate flexural testing. *Dent Mater.* 2004;20:51-62.
  
28. Gonzaga CC, Cesar PF, Miranda WG, Jr., Yoshimura HN. Determination of the slow crack growth susceptibility coefficient of dental ceramics using different methods. *J Biomed Mater Res B Appl Biomater.* 2011;99:247-57.
  
29. McCool JI, Boberick KG, Baran GR. Lifetime predictions for resin-based composites using cyclic and dynamic fatigue. *J Biomed Mater Res.* 2001;58:247-53.
  
30. Bogacki RE, Hunt RJ, del Aguila M, Smith WR. Survival analysis of posterior restorations using an insurance claims database. *Oper Dent.* 2002;27:488-92.
  
31. Cunningham J, Mair LH, Foster MA, Ireland RS. Clinical evaluation of three posterior composite and two amalgam restorative materials: 3-year results. *Br Dent J.* 1990;169:319-23.
  
32. Tyas MJ, Jones DW, Rizkalla AS. The evaluation of resin composite consistency. *Dent Mater.* 1998;14:424-8.

33. Lynch CD, Frazier KB, McConnell RJ, Blum IR, Wilson NH. Minimally invasive management of dental caries: contemporary teaching of posterior resin-based composite placement in U.S. and Canadian dental schools. *J Am Dent Assoc.* 2011;142:612-20.
34. Opdam NJ, Bronkhorst EM, Loomans BA, Huysmans MC. 12-year survival of composite vs. amalgam restorations. *J Dent Res.* 2010;89:1063-7.
35. Opdam NJ, Bronkhorst EM, Roeters JM, Loomans BA. A retrospective clinical study on longevity of posterior composite and amalgam restorations. *Dent Mater.* 2007;23:2-8.
36. Toh WS, Yap A, Lim SY. In Vitro Biocompatibility of Contemporary Bulk-fill Composites. *Oper Dent.* 2015.
37. Furness A, Tadros MY, Looney SW, Rueggeberg FA. Effect of bulk/incremental fill on internal gap formation of bulk-fill composites. *J Dent.* 2014;42:439-49.
38. Costa SXS GM, Jacomass DP, Bernardi MIB, Hernandez AC, Rastelli ANS, Andrade MF. . Continuous and gradual photo-activation methods: influence on degree of conversion and crosslink density of composite resins. . *J Ther Anal Calorim.* 2011;103:219-27.
39. Moraes LG, Rocha RS, Menegazzo LM, de Araujo EB, Yukimito K, Moraes JC. Infrared spectroscopy: a tool for determination of the degree of conversion in dental composites. *J Appl Oral Sci.* 2008;16:145-9.
40. Rastelli ANS JD, Bagnato VS. . Degree of conversion and temperature increase of a composite resin light-cured with argon laser and blue LED. *Las Phys.* 2008;18:1570-5.

41. Ferracane JL. Correlation between hardness and degree of conversion during the setting reaction of unfilled dental restorative resins. *Dent Mater.* 1985;1:11-4.
42. Ferracane JL, Greener EH. The effect of resin formulation on the degree of conversion and mechanical properties of dental restorative resins. *J Biomed Mater Res.* 1986;20:121-31.
43. Hofmann N, Renner J, Hugo B, Klaiber B. Elution of leachable components from resin composites after plasma arc vs standard or soft-start halogen light irradiation. *J Dent.* 2002;30:223-32.
44. Yoon TH, Lee YK, Lim BS, Kim CW. Degree of polymerization of resin composites by different light sources. *J Oral Rehabil.* 2002;29:1165-73.
45. Chung KH. The relationship between composition and properties of posterior resin composites. *J Dent Res.* 1990;69:852-6.
46. Poskus LT, Placido E, Cardoso PE. Influence of placement techniques on Vickers and Knoop hardness of class II composite resin restorations. *Dent Mater.* 2004;20:726-32.
47. Alrahlah A, Silikas N, Watts DC. Post-cure depth of cure of bulk fill dental resin-composites. *Dent Mater.* 2014;30:149-54.
48. Miletic V, Santini A. Optimizing the concentration of 2,4,6-trimethylbenzoyldiphenylphosphine oxide initiator in composite resins in relation to monomer conversion. *Dent Mater J.* 2012;31:717-23.

49. Turssi CP, Ferracane JL, Vogel K. Filler features and their effects on wear and degree of conversion of particulate dental resin composites. *Biomaterials*. 2005;26:4932-7.
50. Tarle Z, Meniga A, Ristic M, Sutalo J, Pichler G, Davidson CL. The effect of the photopolymerization method on the quality of composite resin samples. *J Oral Rehabil*. 1998;25:436-42.
51. Uctasli S, Tezvergil A, Lassila LV, Vallittu PK. The degree of conversion of fiber-reinforced composites polymerized using different light-curing sources. *Dent Mater*. 2005;21:469-75.
52. Fleming GJ, Awan M, Cooper PR, Sloan AJ. The potential of a resin-composite to be cured to a 4mm depth. *Dent Mater*. 2008;24:522-9.
53. Lassila LV, Nagas E, Vallittu PK, Garoushi S. Translucency of flowable bulk-filling composites of various thicknesses. *Chin J Dent Res*. 2012;15:31-5.
54. Flury S, Hayoz S, Peutzfeldt A, Husler J, Lussi A. Depth of cure of resin composites: is the ISO 4049 method suitable for bulk fill materials? *Dent Mater*. 2012;28:521-8.
55. Bucuta S, Ilie N. Light transmittance and micro-mechanical properties of bulk fill vs. conventional resin based composites. *Clin Oral Investig*. 2014;18:1991-2000.
56. Tarle Z, Attin T, Marovic D, Andermatt L, Ristic M, Taubock TT. Influence of irradiation time on subsurface degree of conversion and microhardness of high-viscosity bulk-fill resin composites. *Clin Oral Investig*. 2015;19:831-40.

57. Yu B, Lee YK. Differences in color, translucency and fluorescence between flowable and universal resin composites. *J Dent.* 2008;36:840-6.
58. Shortall AC. How light source and product shade influence cure depth for a contemporary composite. *J Oral Rehabil.* 2005;32:906-11.
59. Zorzin J, Maier E, Harre S, Fey T, Belli R, Lohbauer U, et al. Bulk-fill resin composites: polymerization properties and extended light curing. *Dent Mater.* 2015;31:293-301.
60. Lee YK. Influence of filler on the difference between the transmitted and reflected colors of experimental resin composites. *Dent Mater.* 2008;24:1243-7.
61. Pianelli C, Devaux J, Bebelman S, Leloup G. The micro-Raman spectroscopy, a useful tool to determine the degree of conversion of light-activated composite resins. *J Biomed Mater Res.* 1999;48:675-81.
62. Stansbury JW, Dickens SH. Determination of double bond conversion in dental resins by near infrared spectroscopy. *Dent Mater.* 2001;17:71-9.
63. Ivoclar. V. Scientific Documentation Tetric Evo Ceram Bulk Fill. 2013. .
64. Dentsply. D. SureFil SDR Flow Scientific Compendium. 2009.
65. Kulzer H. Venus Bulk Fill Scientific Compendium 2011.



66. 3M ESPE. Filtek™ Bulk Fill Flowable Restorative 2014.
67. Kleverlaan CJ, Feilzer AJ. Polymerization shrinkage and contraction stress of dental resin composites. *Dent Mater.* 2005;21:1150-7.
68. Braga RR, Ballester RY, Ferracane JL. Factors involved in the development of polymerization shrinkage stress in resin-composites: a systematic review. *Dent Mater.* 2005;21:962-70.
69. Ferracane JL. Developing a more complete understanding of stresses produced in dental composites during polymerization. *Dent Mater.* 2005;21:36-42.
70. Ferracane JL, Mitchem JC. Relationship between composite contraction stress and leakage in Class V cavities. *Am J Dent.* 2003;16:239-43.
71. Braga RR, Ferracane JL. Alternatives in polymerization contraction stress management. *Crit Rev Oral Biol Med.* 2004;15:176-84.
72. Ilie N, Hickel R. Investigations on a methacrylate-based flowable composite based on the SDR technology. *Dent Mater.* 2011;27:348-55.
73. Ilie N, Hickel R. Resin composite restorative materials. *Aust Dent J.* 2011;56 Suppl 1:59-66.
74. Ilie N, Jelen E, Clementino-Luedemann T, Hickel R. Low-shrinkage composite for dental application. *Dent Mater J.* 2007;26:149-55.

75. Tantbirojn D, Pfeifer CS, Braga RR, Versluis A. Do low-shrink composites reduce polymerization shrinkage effects? *J Dent Res.* 2011;90:596-601.
76. Van Ende A, Mine A, De Munck J, Poitevin A, Van Meerbeek B. Bonding of low-shrinking composites in high C-factor cavities. *J Dent.* 2012;40:295-303.
77. Rode KM, Kawano Y, Turbino ML. Evaluation of curing light distance on resin composite microhardness and polymerization. *Oper Dent.* 2007;32:571-8.
78. Lovell LG, Lu H, Elliott JE, Stansbury JW, Bowman CN. The effect of cure rate on the mechanical properties of dental resins. *Dent Mater.* 2001;17:504-11.
79. Ak AT, Alpoz AR, Bayraktar O, Ertugrul F. Monomer Release from Resin Based Dental Materials Cured With LED and Halogen Lights. *Eur J Dent.* 2010;4:34-40.
80. Jandt KD, Mills RW, Blackwell GB, Ashworth SH. Depth of cure and compressive strength of dental composites cured with blue light emitting diodes (LEDs). *Dent Mater.* 2000;16:41-7.
81. Roberts HW, Vandewalle KS, Berzins DW, Charlton DG. Accuracy of LED and halogen radiometers using different light sources. *J Esthet Restor Dent.* 2006;18:214-22; discussion 23-4.
82. Davidson CL, Feilzer AJ. Polymerization shrinkage and polymerization shrinkage stress in polymer-based restoratives. *J Dent.* 1997;25:435-40.
83. Puckett AD, Smith R. Method to measure the polymerization shrinkage of light-cured composites. *J Prosthet Dent.* 1992;68:56-8.

84. Labella R, Lambrechts P, Van Meerbeek B, Vanherle G. Polymerization shrinkage and elasticity of flowable composites and filled adhesives. *Dent Mater.* 1999;15:128-37.

85. Norris C BJ. Polymerization shrinkage of seventeen composite resins [abstract]. *J Dent Res* 2002;;81.

86. Surefil SDR brochure product. Dentsply international. 2010.

87. Burgess J, Cakir D. Comparative properties of low-shrinkage composite resins. *Compend Contin Educ Dent.* 2010;31 Spec No 2:10-5.

88. Giachetti L, Bertini F, Bambi C, Scaminaci Russo D. A rational use of dental materials in posterior direct resin restorations in order to control polymerization shrinkage stress. *Minerva Stomatol.* 2007;56:129-38.

89. Scientific Compendium SDR Polymerization shrinkage and stress 2011 [cited 2013 11,05,2013]. Available from: <http://www.dentsplymea.com/sites/default/files/Scientific%20compendium%20SDR%20-%202011>.

90. Tomaszewska IM, Kearns JO, Ilie N, Fleming GJ. Bulk fill restoratives: to cap or not to cap--that is the question? *J Dent.* 2015;43:309-16.

91. McCulloch AJ, Smith BG. In vitro studies of cusp reinforcement with adhesive restorative material. *Br Dent J.* 1986;161:450-2.

92. Alomari QD, Reinhardt JW, Boyer DB. Effect of liners on cusp deflection and gap formation in composite restorations. *Oper Dent.* 2001;26:406-11.
93. Asmussen E. Restorative resins: hardness and strength vs. quantity of remaining double bonds. *Scand J Dent Res.* 1982;90:484-9.
94. Cohen ME, Leonard DL, Charlton DG, Roberts HW, Ragain JC. Statistical estimation of resin composite polymerization sufficiency using microhardness. *Dent Mater.* 2004;20:158-66.
95. Soh MS, Yap AU, Siow KS. The effectiveness of cure of LED and halogen curing lights at varying cavity depths. *Oper Dent.* 2003;28:707-15.
96. Amber Tiba PGGZ, DDS,MS; Cameron Estrich, MPH; Albert Hong. A Laboratory Evaluation of Bulk-fill Versus Traditional Multi-Increment-Fill Resin-Based Composites. *ADA Professional Product Review.* 2013;8:13-25.
97. Finan L, Palin WM, Moskwa N, McGinley EL, Fleming GJ. The influence of irradiation potential on the degree of conversion and mechanical properties of two bulk-fill flowable RBC base materials. *Dent Mater.* 2013;29:906-12.
98. Ilie N, Kessler A, Durner J. Influence of various irradiation processes on the mechanical properties and polymerisation kinetics of bulk-fill resin based composites. *J Dent.* 2013;41:695-702.
99. Leprince J, Palin WM, Mullier T, Devaux J, Vreven J, Leloup G. Investigating filler morphology and mechanical properties of new low-shrinkage resin composite types. *J Oral Rehabil.* 2010;37:364-76.

100. Goracci C, Cadenaro M, Fontanive L, Giangrosso G, Juloski J, Vichi A, et al. Polymerization efficiency and flexural strength of low-stress restorative composites. *Dent Mater.* 2014;30:688-94.
101. Quinn JB, Quinn GD. A practical and systematic review of Weibull statistics for reporting strengths of dental materials. *Dent Mater.* 2010;26:135-47.
102. Ferracane JL. Resin-based composite performance: are there some things we can't predict? *Dent Mater.* 2013;29:51-8.
103. Ibrahim WM, McCabe JF. The use of Weibull statistics in mechanical testing of brittle dental materials. *J Nihon Univ Sch Dent.* 1993;35:225-9.
104. Ritter JE. Predicting lifetimes of materials and material structures. *Dent Mater.* 1995;11:142-6.
105. Tinschert J, Zvez D, Marx R, Anusavice KJ. Structural reliability of alumina-, feldspar-, leucite-, mica- and zirconia-based ceramics. *J Dent.* 2000;28:529-35.
106. P. Kittl GD. Weibull fracture statistics or probabilistic strength of materials. *Res Mechanica.* 1988;24:99-207.
107. Weibull. W. A statistical distribution function of wide applicability. *J Appl Mech.* 1951;18:293-7.

108. Tjandrawinata R, Irie M, Suzuki K. Flexural properties of eight flowable light-cured restorative materials, in immediate vs 24-hour water storage. *Oper Dent.* 2005;30:239-49.
109. Butikofer L, Stawarczyk B, Roos M. Two regression methods for estimation of a two-parameter Weibull distribution for reliability of dental materials. *Dent Mater.* 2015;31:e33-50.
110. Morena R, Beaudreau GM, Lockwood PE, Evans AL, Fairhurst CW. Fatigue of dental ceramics in a simulated oral environment. *J Dent Res.* 1986;65:993-7.
111. Ohyama T, Yoshinari M, Oda Y. Effects of cyclic loading on the strength of all-ceramic materials. *Int J Prosthodont.* 1999;12:28-37.
112. Studart AR, Filser F, Kocher P, Gauckler LJ. Fatigue of zirconia under cyclic loading in water and its implications for the design of dental bridges. *Dent Mater.* 2007;23:106-14.
113. Drummond JL. Degradation, fatigue, and failure of resin dental composite materials. *J Dent Res.* 2008;87:710-9.
114. Lin J, Sun M, Zheng Z, Shinya A, Han J, Lin H, et al. Effects of rotating fatigue on the mechanical properties of microhybrid and nanofiller-containing composites. *Dent Mater J.* 2013;32:476-83.
115. Lohbauer U, Belli R, Ferracane JL. Factors involved in mechanical fatigue degradation of dental resin composites. *J Dent Res.* 2013;92:584-91.
116. Soderholm KJ, Roberts MJ. Influence of water exposure on the tensile strength of composites. *J Dent Res.* 1990;69:1812-6.

117. Braem MJ, Lambrechts P, Gladys S, Vanherle G. In vitro fatigue behavior of restorative composites and glass ionomers. *Dent Mater.* 1995;11:137-41.
118. Chen HY, Hickel R, Setcos JC, Kunzelmann KH. Effects of surface finish and fatigue testing on the fracture strength of CAD-CAM and pressed-ceramic crowns. *J Prosthet Dent.* 1999;82:468-75.
119. Benaqqa C, Chevalier J, Saadaoui M, Fantozzi G. Slow crack growth behaviour of hydroxyapatite ceramics. *Biomaterials.* 2005;26:6106-12.
120. Reese MJ CJ. Delayed failure/subcritical crack growth of ceramics. National Physical Laboratory. 1992:4-30.
121. Drummond JL. Cyclic fatigue of composite restorative materials. *J Oral Rehabil.* 1989;16:509-20.
122. Belli R, Geinzer E, Muschweck A, Petschelt A, Lohbauer U. Mechanical fatigue degradation of ceramics versus resin composites for dental restorations. *Dent Mater.* 2014;30:424-32.
123. Belli R, Petschelt A, Lohbauer U. Are linear elastic material properties relevant predictors of the cyclic fatigue resistance of dental resin composites? *Dent Mater.* 2014;30:381-91.
124. Zhu Q, de With G, Dortmans LJ, Feenstra F. Subcritical crack growth behavior of Al<sub>2</sub>O<sub>3</sub>-glass dental composites. *J Biomed Mater Res B Appl Biomater.* 2003;65:233-8.

125. Fairhurst CW, Lockwood PE, Ringle RD, Twiggs SW. Dynamic fatigue of feldspathic porcelain. *Dent Mater.* 1993;9:269-73.
126. Lohbauer U, Petschelt A, Greil P. Lifetime prediction of CAD/CAM dental ceramics. *J Biomed Mater Res.* 2002;63:780-5.
127. Teixeira EC, Piascik JR, Stoner BR, Thompson JY. Dynamic fatigue and strength characterization of three ceramic materials. *J Mater Sci Mater Med.* 2007;18:1219-24.
128. Borba M, de Araujo MD, Fukushima KA, Yoshimura HN, Cesar PF, Griggs JA, et al. Effect of the microstructure on the lifetime of dental ceramics. *Dent Mater.* 2011;27:710-21.
129. Bayne SC. Correlation of clinical performance with 'in vitro tests' of restorative dental materials that use polymer-based matrices. *Dent Mater.* 2012;28:52-71.
130. C1368-00. A. Standard test method for determination of slow crack growth parameters of advanced ceramics by constant stress-rate flexural testing at ambient temperature. . American Society for Testing and Materials 2001.
131. ISO 6872. Dentistry – dental ceramics. International Organization for Standards; . 1999.
132. Chung SM, Yap AU, Koh WK, Tsai KT, Lim CT. Measurement of Poisson's ratio of dental composite restorative materials. *Biomaterials.* 2004;25:2455-60.



133. C1239. A. Reporting uniaxial strength data and estimating Weibull distribution parameters for advanced ceramics. American Society for Testing Materials ;. 2000.
134. Davidge RW MJ, Tappin G. . Strength–probability–time (SPT) relationships in ceramics. Journal of Materials Science. 1973;;8:1699–705.
- .
135. Lohbauer U, von der Horst T, Frankenberger R, Kramer N, Petschelt A. Flexural fatigue behavior of resin composite dental restoratives. Dent Mater. 2003;19:435-40.
136. Gonzaga CC, Cesar PF, Miranda WG, Jr., Yoshimura HN. Slow crack growth and reliability of dental ceramics. Dent Mater. 2011;27:394-406.
137. Ortengren U, Wellendorf H, Karlsson S, Ruyter IE. Water sorption and solubility of dental composites and identification of monomers released in an aqueous environment. J Oral Rehabil. 2001;28:1106-15.
138. Loughran GM, Versluis A, Douglas WH. Evaluation of sub-critical fatigue crack propagation in a restorative composite. Dent Mater. 2005;21:252-61.
139. Q G. Fractography of ceramics and glasses. . Government Printing Office, Washington. 2007.
140. Ferracane JL, Berge HX, Condon JR. In vitro aging of dental composites in water--effect of degree of conversion, filler volume, and filler/matrix coupling. J Biomed Mater Res. 1998;42:465-72.

141. Lohbauer U, Kramer N, Petschelt A, Frankenberger R. Correlation of in vitro fatigue data and in vivo clinical performance of a glassceramic material. Dent Mater. 2008;24:39-44.
142. Mitov G, Lohbauer U, Rabbo MA, Petschelt A, Pospiech P. Investigations of subcritical crack propagation of the Empress 2 all-ceramic system. Dent Mater. 2008;24:267-73.
143. Kim KH, Ong JL, Okuno O. The effect of filler loading and morphology on the mechanical properties of contemporary composites. J Prosthet Dent. 2002;87:642-9.